Jet Flavor Probes of QGP @ RHIC and LHC

M. Gyulassy 12/05/13 NFQCD @ YITP

Jet Flavor Probes of QGP @ RHIC and LHC

M. Gyulassy 12/05/13 NFQCD @ YITP

1) **QCD Tomography** vs **AdS Holography**

2) **Tomography** with **CUJET2.0** = rcDGLV + VISH(2+1)
J. Xu, A.Buzzatti, M.G., in preparation

3) **Holography** with "Shooting Strings"
A. Ficnar, S. Gubser, M.G., arXiv:1311.6160 [hep-ph]

Collabs: Barbara Betz, Alessandro Buzzatti, Andrej Ficnar, Steven Gubser, Jorge Noronha, Giorgio Torrieri, Jiechen Xu. +(Djordjevic, Horowitz, Wicks, Levai, Vitev)

Jet quenching vs. η/s

From B. Mueller's Theory Overview talk 12/2/13

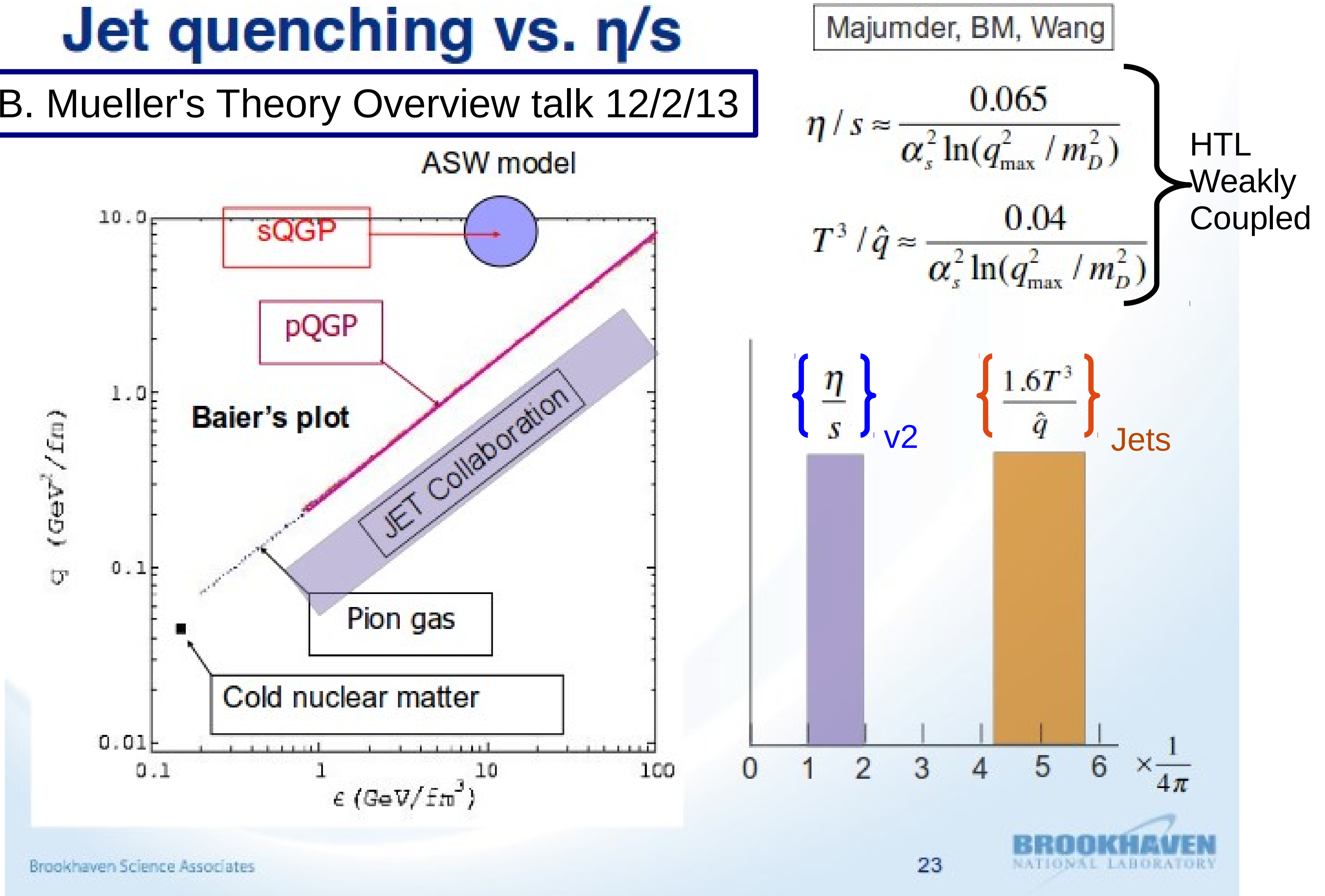

Bulk Flow suggests strongly coupled near "perfect fluidity" for pT<2 GeV while Hard Jet probes suggest weak jet medium interactions pT>10.

30 Years of A+A data: "The Big Picture" from SPS to LHC

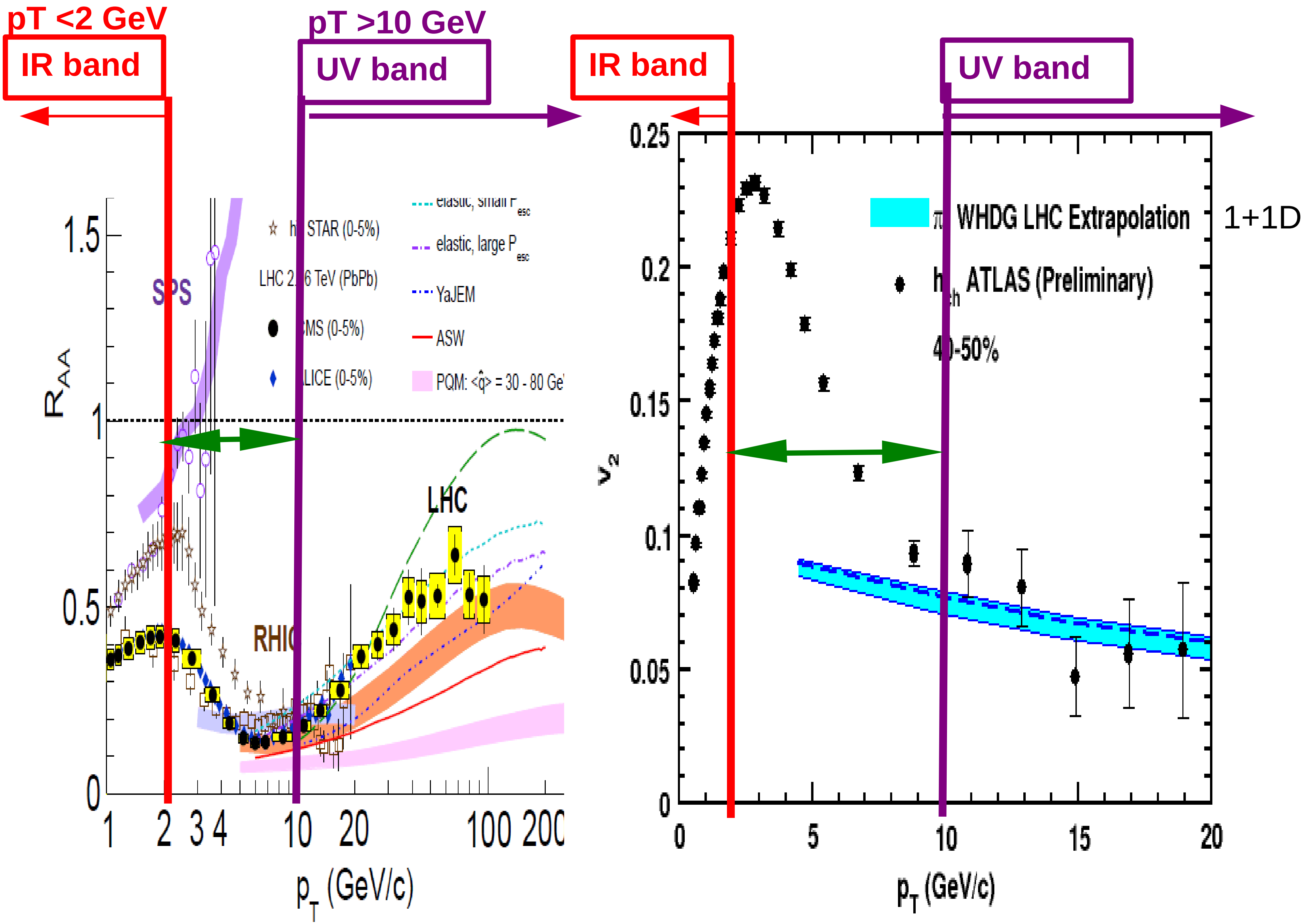

The physics in the IR seems clearly different from the UV.

pQCD Tomography vs hQCD Holography (vs CGC Geneology)

Getting to the bottom of the heavy quark jet puzzle

M.Gyulassy
Physics **2**, 107 (2009)

DGLV
BDMPS
ASW
WHDG
CUJET
ZLCPI
AMY
HT

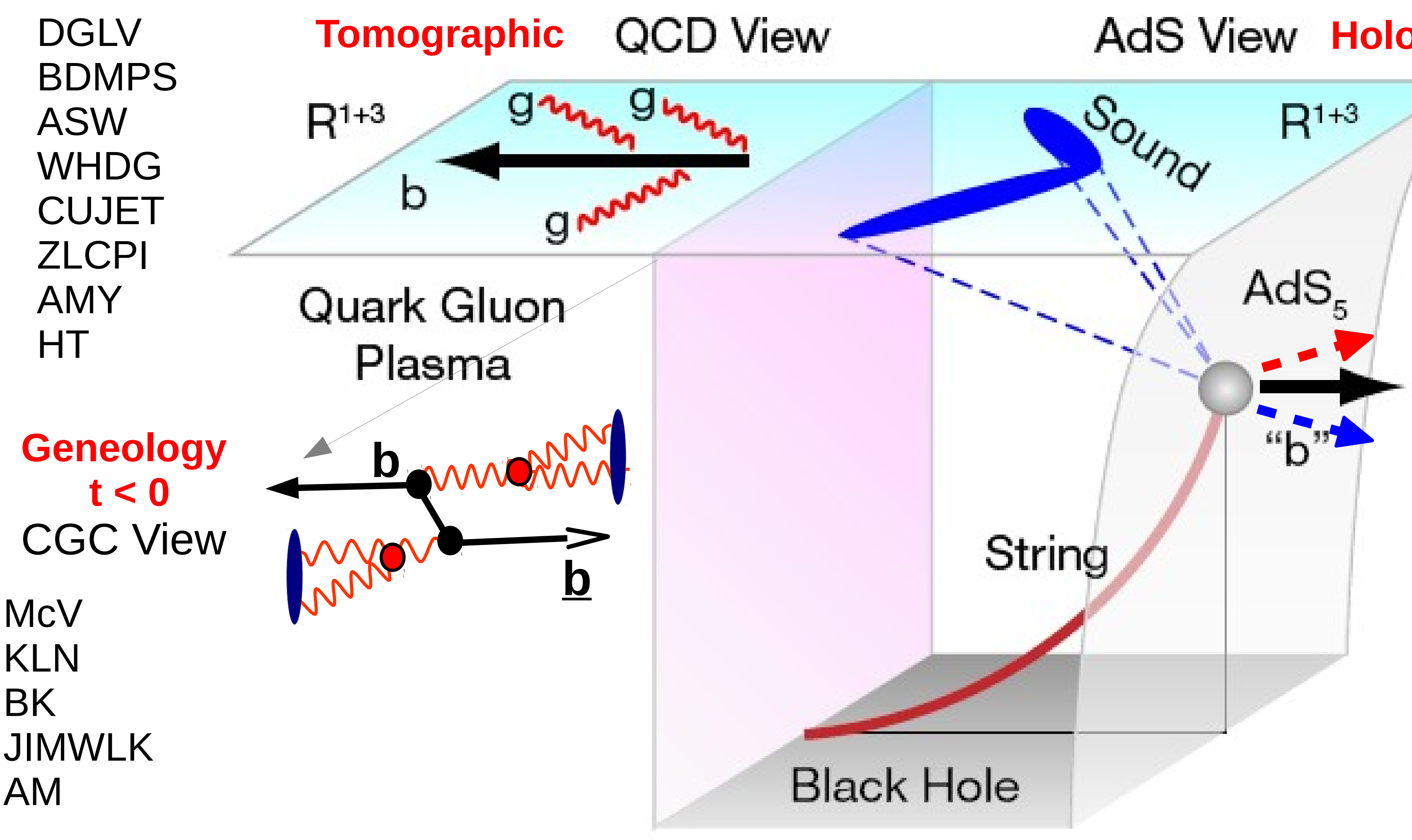

Herzog ..
Gubser ..
Chesler ..

HG
NGT
BNGT
NFG
FSG

McV
KLN
BK
JIMWLK
AM

Which paradigm can best account for Jet Quenching observables at RHIC and LHC?

Jet Tomo vs Jet Holo in 2013

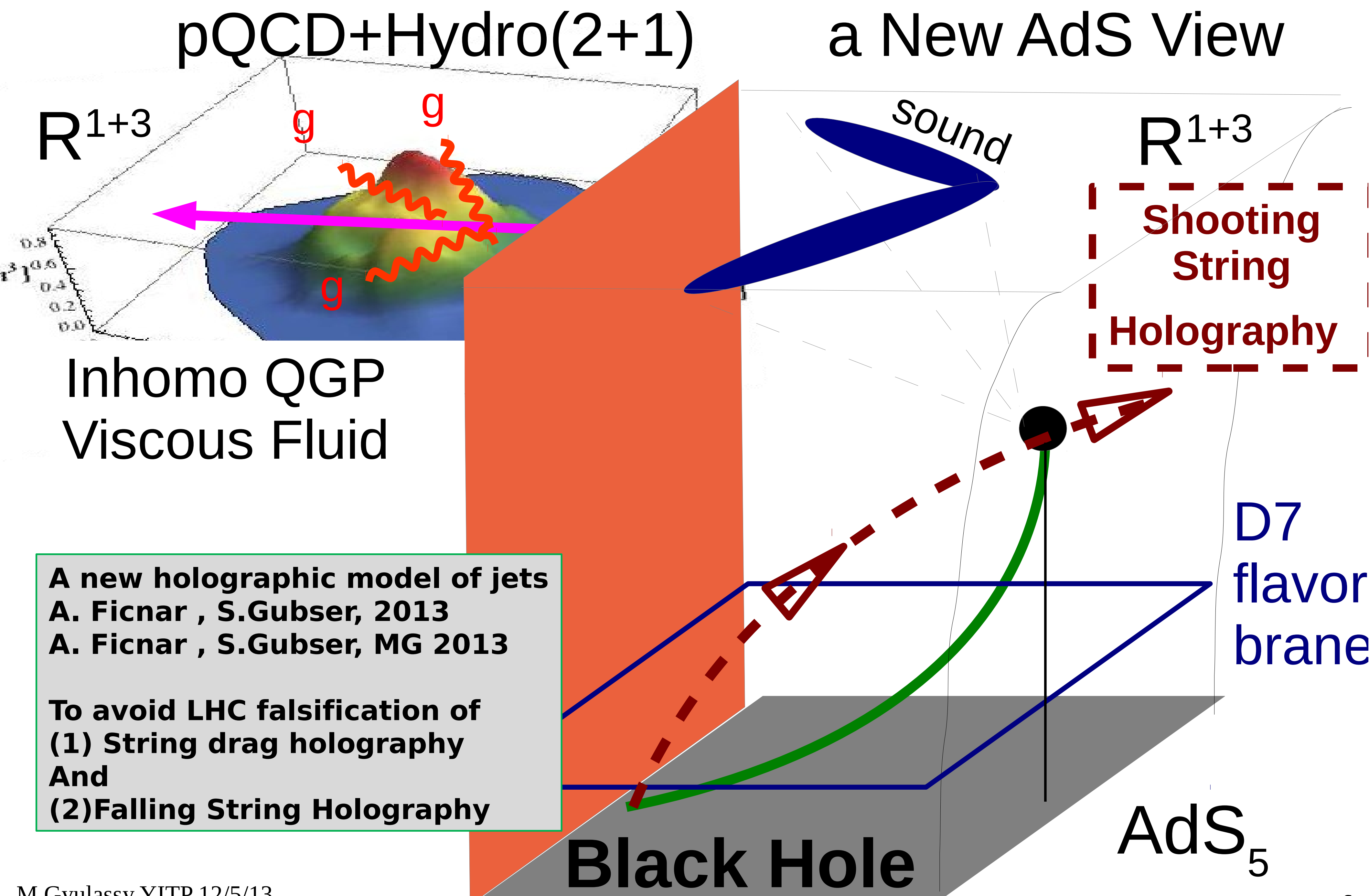

A new holographic model of jets
A. Ficnar , S.Gubser, 2013
A. Ficnar , S.Gubser, MG 2013

To avoid LHC falsification of
(1) String drag holography
And
(2)Falling String Holography

DGLV model

Running coupling

$\alpha\left(k_T^2/(x(1-x))\right)$

$\left(\alpha\left(q_i^2\right)\right)^2$

$$x\frac{dN^{(n)}}{dx\,d^2\mathbf{k}} = \frac{C_R\alpha_s}{\pi^2}\frac{1}{n!}\int\prod_{i=1}^{n}\left(d^2\mathbf{q}_i\frac{L}{\lambda_g(i)}\left[\bar{v}_i^2(\mathbf{q}_i)-\delta^2(\mathbf{q}_i)\right]\right)\times$$

$$\times\left(-2\,\tilde{\mathbf{C}}_{(1,\cdots,n)}\cdot\sum_{m=1}^{n}\tilde{\mathbf{B}}_{(m+1,\cdots,n)(m,\cdots,n)}\left[\cos\left(\sum_{k=2}^{m}\Omega_{(k,\cdots,n)}\Delta z_k\right)-\cos\left(\sum_{k=1}^{m}\Omega_{(k,\cdots,n)}\Delta z_k\right)\right]\right)$$

$\alpha\left(9T^2\right)$

Soft Radiation ($E \gg \omega,\ x \ll 1$)
Soft Scattering ($E \gg q,\ \omega \gg k_T$)

Opacity series expantion $\longrightarrow$ $\left(\frac{L}{\lambda}\right)^n$

Radiation antenna $\longrightarrow$ *Cascade terms*

$$\tilde{\mathbf{C}}_{(i_1 i_2\cdots i_m)} = \frac{(\mathbf{k}-\mathbf{q}_{i_1}-\mathbf{q}_{i_2}-\cdots-\mathbf{q}_{i_m})}{(\mathbf{k}-\mathbf{q}_{i_1}-\mathbf{q}_{i_2}-\cdots-\mathbf{q}_{i_m})^2+m_g^2+M^2x^2},$$

$$\tilde{\mathbf{B}}_{(i_1 i_2\cdots i_m)(j_1 j_2\cdots j_n)} = \tilde{\mathbf{C}}_{(i_1 i_2\cdots j_m)}-\tilde{\mathbf{C}}_{(j_1 j_2\cdots j_n)}.$$

Gunion – Bertsch $\quad \tilde{\mathbf{B}}_i = \tilde{\mathbf{H}}-\tilde{\mathbf{C}}_i\,,$

Hard $\quad \tilde{\mathbf{H}} = \frac{\mathbf{k}}{\mathbf{k}^2+m_g^2+M^2x^2},$

$\alpha\left(9T^2\right)$

LPM effect $\longrightarrow$

$$\Omega_{(m,\cdots,n)} = \underbrace{\frac{(\mathbf{k}-\mathbf{q}_m-\cdots-\mathbf{q}_n)^2}{2xE}}_{\textit{Inverse formation time}}+\underbrace{\frac{m_g^2+M^2x^2}{2xE}}_{\textit{Mass effects}}$$

Scattering center distribution $\longrightarrow$ $\Delta z_k = z_k - z_{k-1} \sim L/(n+1)$

Multi-scale running coupling

- Introduce one-loop alpha running

$$\alpha_s \to \alpha_s(Q^2)\begin{cases} \alpha_0 & if\ Q \le Q_0 \\ \dfrac{2\pi}{9\log(Q/\Lambda)} & if\ Q > Q_0 \end{cases}$$

B. G. Zakharov, JETP Lett. 88 (2008) 781-786

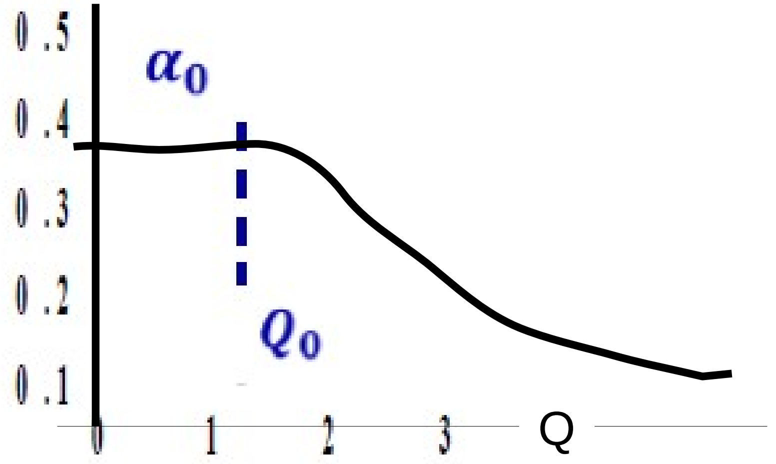

$$Radiative = \begin{cases} \alpha(q^2)^2 \\ \alpha\left(\dfrac{k_\perp^2}{x(1-x)}\right) \\ \mu = g\left(\alpha(2T^2)\right)T \end{cases}$$

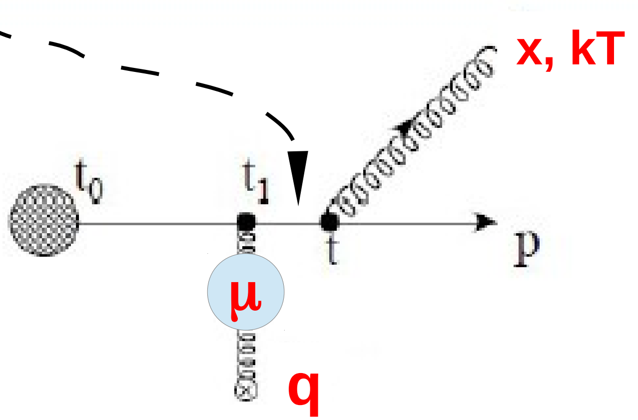

$$Elastic = \begin{cases} \alpha(ET) \\ \alpha(\mu^2) \end{cases}$$

S. Peigne and A. Peshier, Phys.Rev. D77 (2008) 114017

Finite momentum string endpoint holographic action

- Introduce finite endpoint momentum via surface term:

$$S = -\frac{1}{4\pi\alpha'}\int_M d\tau d\sigma \sqrt{-h}h^{ab}\partial_a X^\mu \partial_b X^\nu G_{\mu\nu} + \int_{\partial M} d\xi \frac{1}{2\eta}\dot{X}^\mu \dot{X}^\nu G_{\mu\nu}$$
$$+ \frac{1}{2\kappa_5^2}\int d^5x\sqrt{-G}\left[R + \frac{12}{L^2} + L^2\frac{\lambda_{GB}}{2}\left(R^2 - 4R_{\mu\nu}^2 + R_{\mu\nu\rho\sigma}^2\right)\right]$$

= Nambu-Goto + the New Boundary term + Bulk Geom(R + R^2)

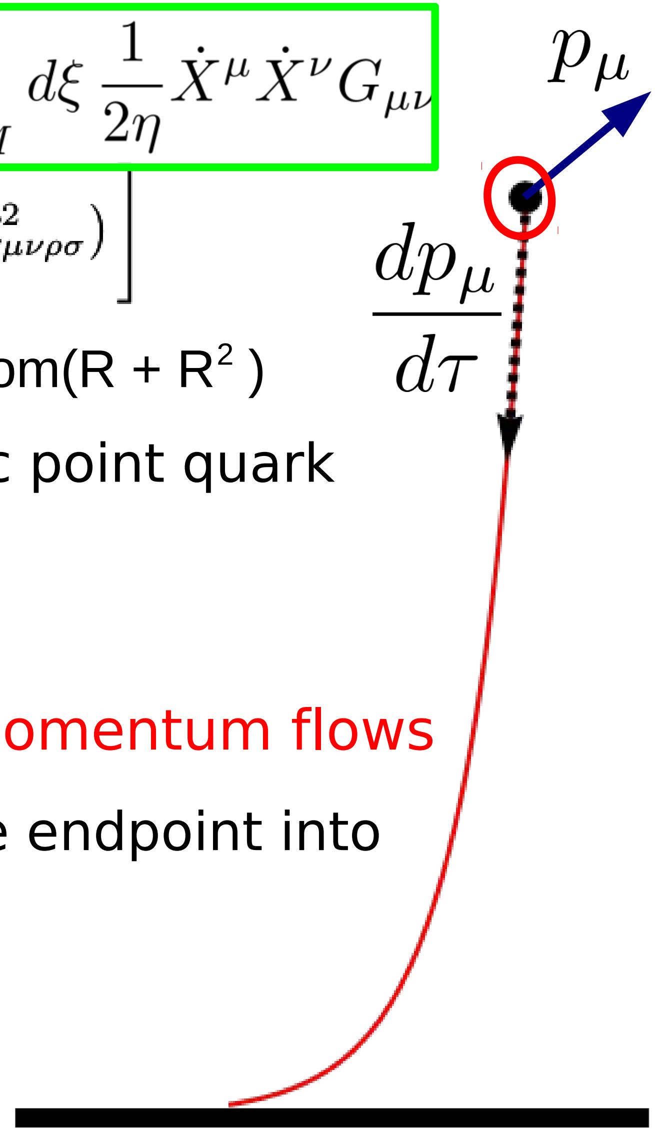

A more natural "Lund"like description of an energetic point quark and its trailing color flux tube:

- Endpoint is the point quark X^μ
- String = its nonlocal "color field" into which momentum flows

- **Unique definition** of the jet energy loss from the endpoint into the bulk of via a string

$$\dot{p}_\mu - \Gamma^\kappa_{\mu\lambda}\dot{X}^\lambda p_\kappa = \mp\frac{\eta}{2\pi\alpha'}p_\mu = \mp\frac{1}{2\pi\alpha'}G_{\mu\nu}\dot{X}^\nu$$

Gubser, Klebanov, Tseytlin (98)
Gubser, PRD74 (06)
Buchel, Myers, Sinha, Paulos (08,09)

Kats, Petrov 07
Brigante 08
Maldacena Hoffman 08

Connecting Hard & Soft Phenomena @ RHIC

J. Noronha, MG, G.Torrieri, hep-ph: 0906.4099, PRC82 (2010) 054903

The idea is to use both $R^2 \propto \lambda_{GB} \sim 1/N_c$ *and* $R^4 \propto \lambda^{-3/2}$ *pertubations* to R^1 (AdS_5)

(1) $$\frac{\eta}{s} = \frac{1}{4\pi}\left(1 - 4\lambda_{GB} + 15\frac{\zeta(3)}{\lambda^{3/2}}\right)$$

(2) $$\frac{s}{s_{SB}} = \frac{3}{4}\left(1 + \lambda_{GB} + \frac{15}{8}\frac{\zeta(3)}{\lambda^{3/2}}\right)$$

Heavy quark energy loss

(3) $$\frac{dp}{dt} = -\frac{\sqrt{\lambda}\pi T^2}{2M_Q}\left(1 + \frac{3}{2}\lambda_{GB} + \frac{15}{16}\frac{\zeta(3)}{\lambda^{3/2}}\right)$$

(4) Nonconformal deformations possible via Dilatons

To compute

$$R_{AA} \times v_2$$

Jet Bulk

Predicts three fold *analytic* correlations between soft thermo, transport, *and* hard nonequilib dynamics!
** Holography's claim to fame **

M.Djordjevic, S. Wicks, MG

Sqrt(s) and M variation of initial jet spectra provide
Powerful experimental nobs to test models

PRL **94,** 112301 (2005)

Open Charm and Beauty at Ultrarelativistic Heavy Ion Colliders

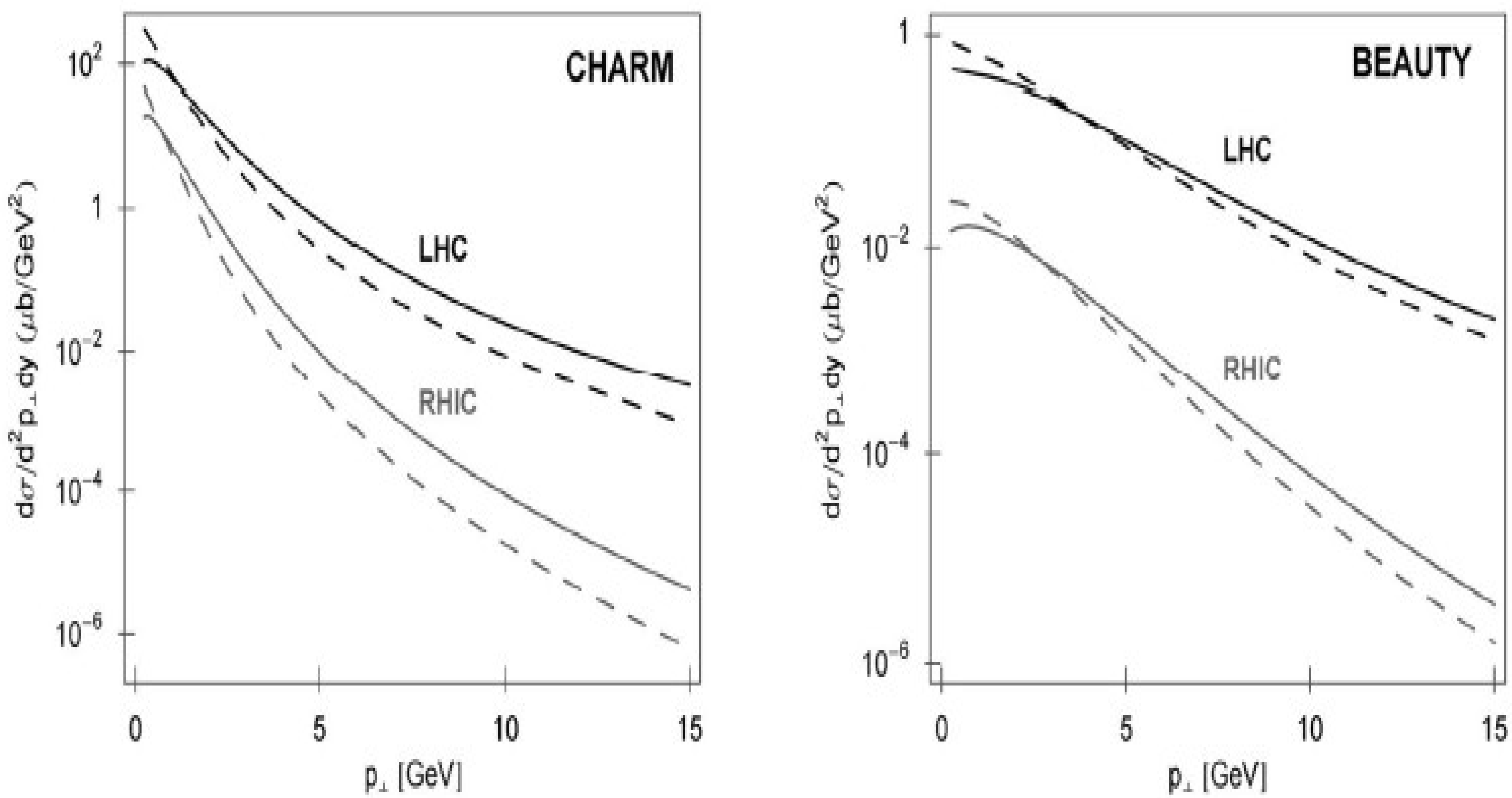

FIG. 1. Initial $p_\perp$ distributions are shown for D (left) and B mesons (right). Lower (upper) curves correspond to the RHIC (LHC) case. Solid curves are computed by assuming δ-function fragmentation, while dashed curves assume Peterson fragmentation [14]. For D (B) mesons we used $\epsilon = 0.06$ ($\epsilon = 0.006$) [13].

(Thanks to R. Vogt with MNR QCD code)

[12] M. L. Mangano, P. Nason, and G. Ridolfi, Nucl. Phys. **B373**, 295 (1992).

CUJET1.0 = rc DGLV (rad + el) + Bj(1+1) QGP

A.Buzzatti, MG, NPA 904 (2013) 779

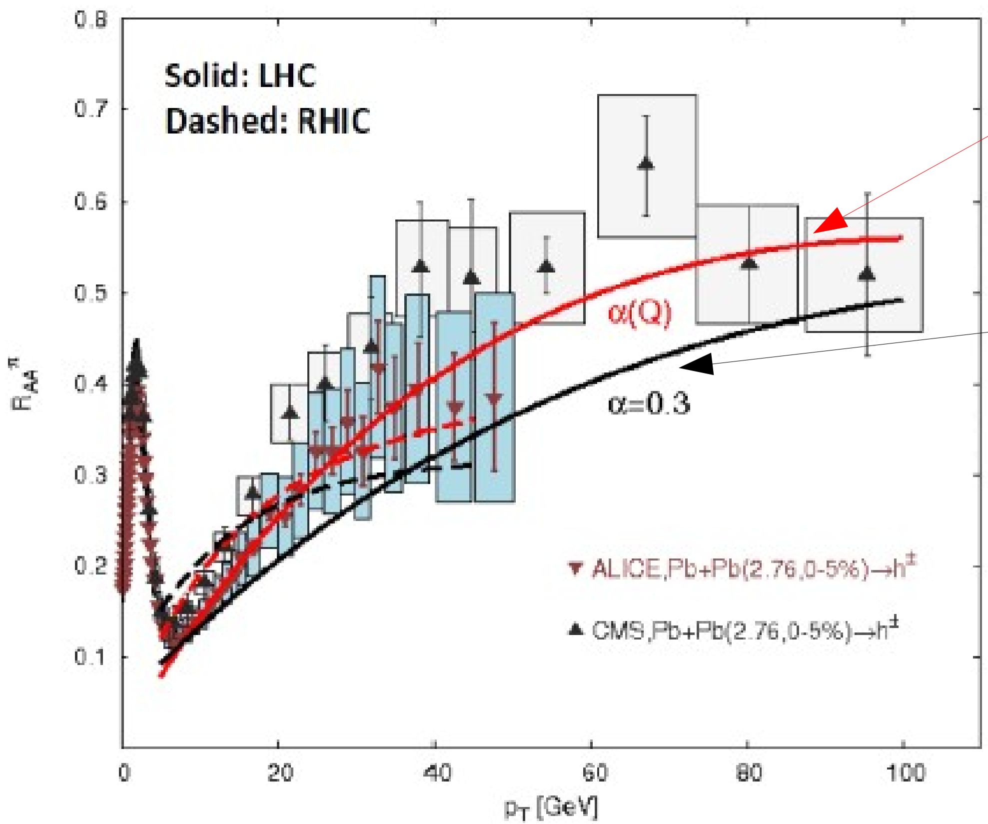

Running coupling *naturally* explains relative transparency LHC QGP At 2 X RHIC density as well as RHIC RAA

(RHIC constrained fixed coupling Over-predicts quenching at LHC)

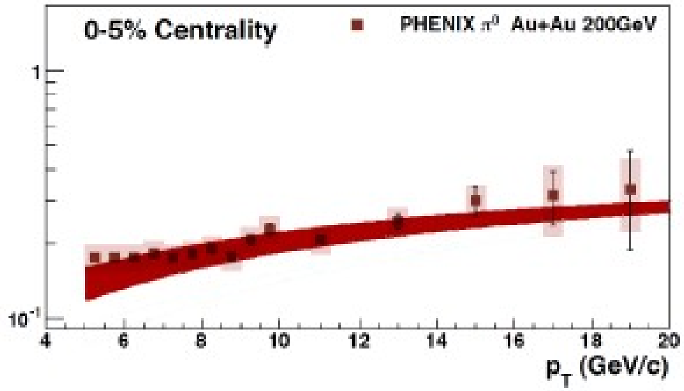

Figure 1: (Left) Pion R_{AA} at LHC (solid lines) and RHIC (dashed lines). In black the fixed coupling CUJET results, constrained at $p_T = 10$ GeV RHIC with $\alpha_s = 0.3$. In red the running coupling CUJET results, constrained at $p_T = 40$ GeV LHC with $\alpha_0 = 0.4$. Central 0% – 5% preliminary ALICE and CMS $h\pm$ LHC data [9] (brown and gray triangles, respectively) are compared to predictions. (Right) Notice the accordance with data [14] of the RHIC Pion R_{AA} running coupling result in the range of energies 5 – 20 GeV.

Higher pT slope of RAA at LHC is due to much harder initial jet spectra ~1/pT^5 That dominates over higher energy loss

Generic "abc" Models of Jet Energy Loss and RAA

For pQCD
fc: a ~ 1/3 , b~1
rc: a ~ 0 , b~1

$$\frac{dP}{d\tau} = -\kappa P^a \tau^b T^{2-a+b}(x(\tau), \tau)$$

For Holographic Falling Strings (Chesler Yaffe)
Lstop ~ $E^{1/3}$
=> a = 1/3 , b=1
OR a = 0 , b=2

$$P_0(P_f) = \left[P_f^{1-a} + K \int_{\tau_0}^{\tau_f} \tau^b \, T^c[\vec{x}_\perp(\tau), \tau] d\tau\right]^{\frac{1}{1-a}},$$

For Holographic String Drag (Gubser, Herzog)
a = 1 , b=0

The new AdS "Shooting String Holography" (Ficnar,Gubser, MG)
=> a=0, b(t) interpolates between b=0 and 2, and c(t)=b(t)+2

$$R_{AA}(p_f; s, A) = \frac{\partial p_0}{\partial p_f} \frac{d\sigma(p_0(p_f))/dp}{d\sigma(p_f)/dp}$$

Spectral index From pQCD

For Bj Brick
$$\approx \left(1 + \kappa' \frac{(dN/dy)^{(2-a+b)/3}}{(Lp_f)^{1-a}}\right)^{\frac{a-n(p_f)}{1-a}}$$

Fix κ' by fit to one RHIC R(pf=10 GeV ,dNdy=1000) reference point.

Horowitz,MG, NPA872(2011); B.Betz, MG, Torrieri PRC84(11), PRC86(12)

CUJET1.0 solved the Non-Photonic Electron quenching puzzle!

A. Buzzatti, MG, PRL 108 (2012)

Jet Flavor Tomography of Quark Gluon Plasmas at RHIC and LHC

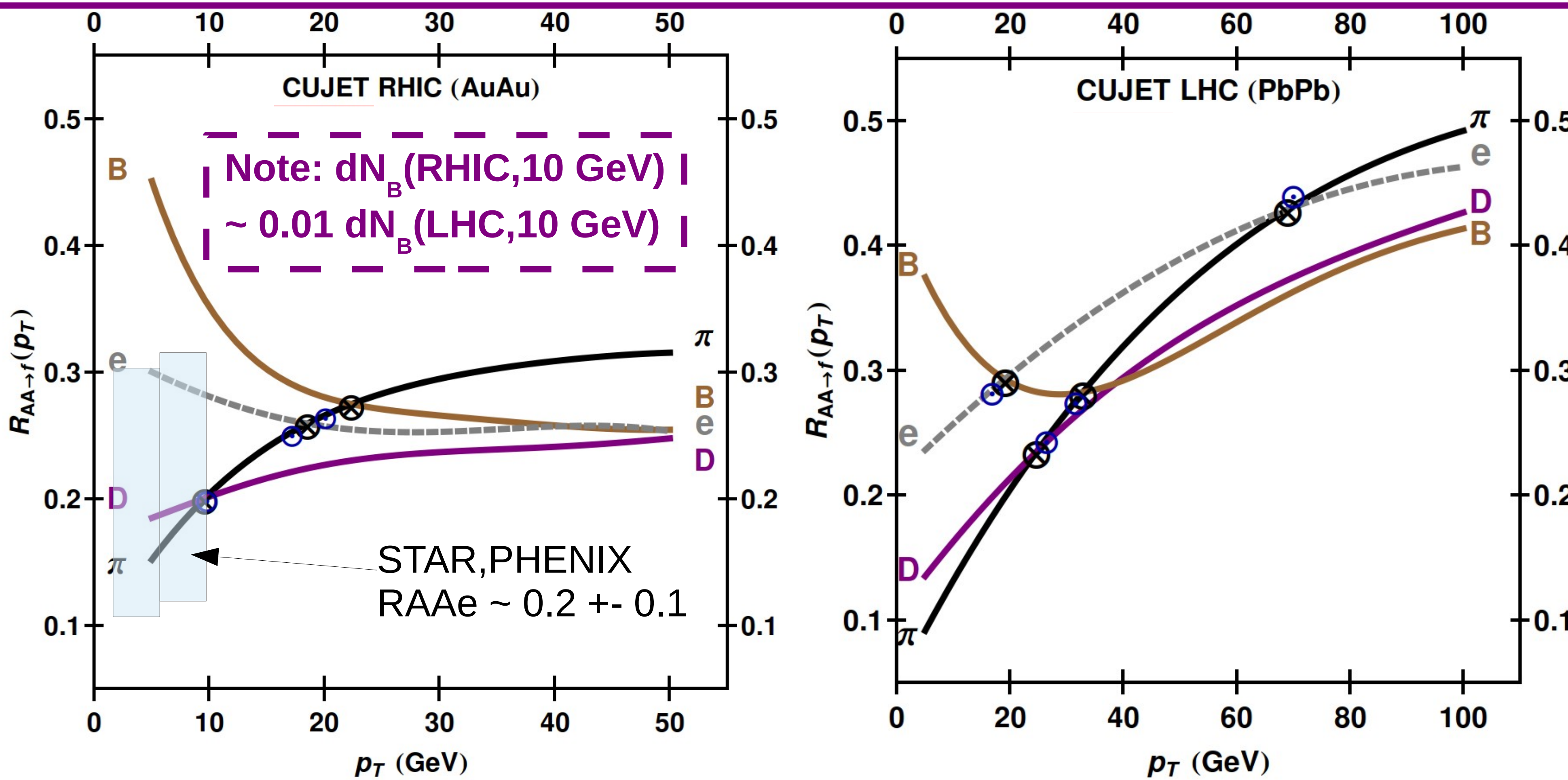

pQCD CUJET Monte Carlo with dynamical scattering predicted

1) a novel quark flavor level crossing pattern at RHIC and LHC

2) and solved the RHIC non-photonic heavy quark puzzle from 2006

3) Exp error bars on NPE currently too large to test RAA level crossing

4) Future Identified B RAA data are essential

Open heavy flavor data

CUJET @ LHC

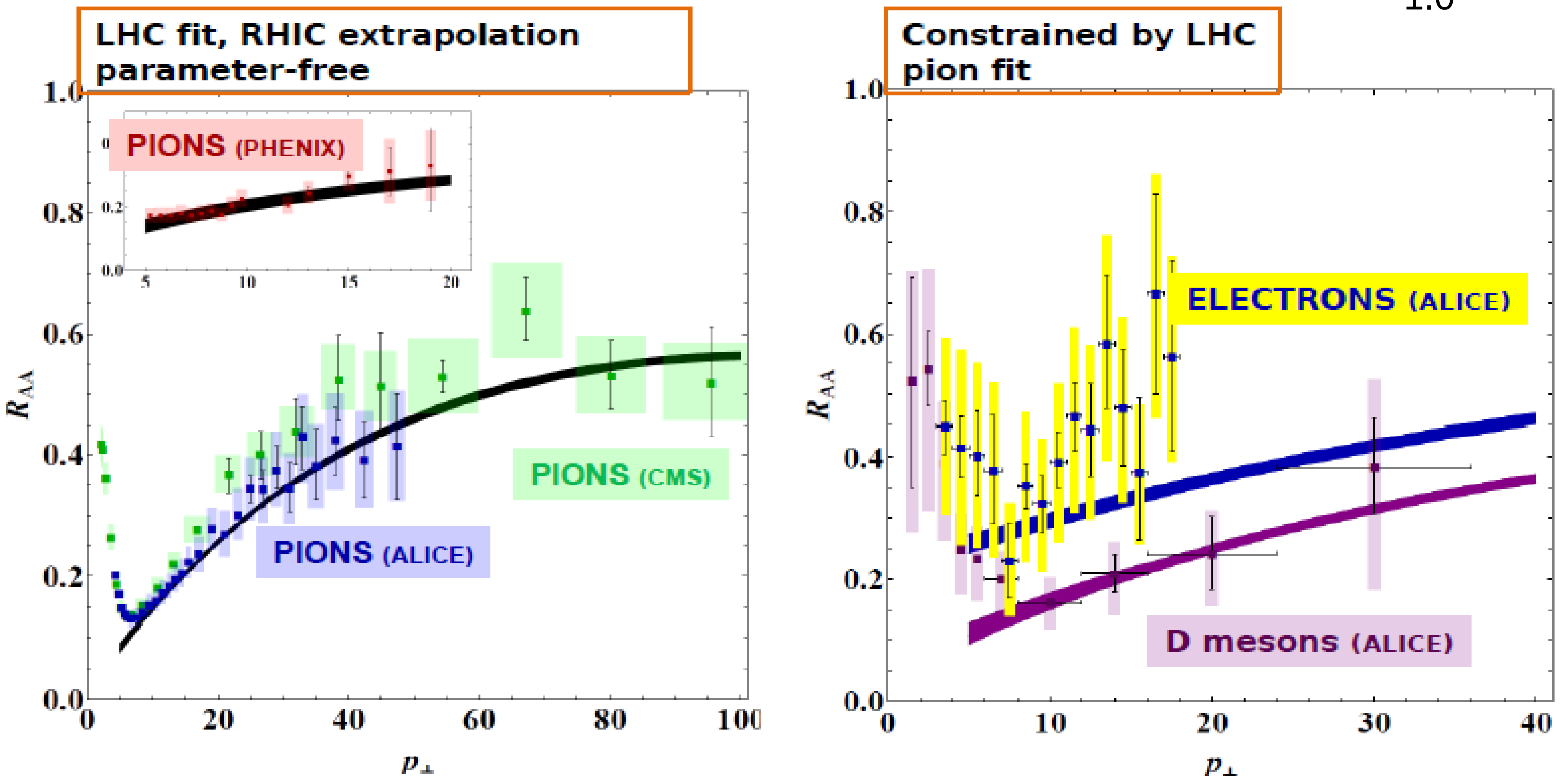

CUJET1.0 = rc DGLV (rad + el) + Bj(1+1) QGP

A.Buzzatti, MG,QM12
NPA 904 (2013) 779

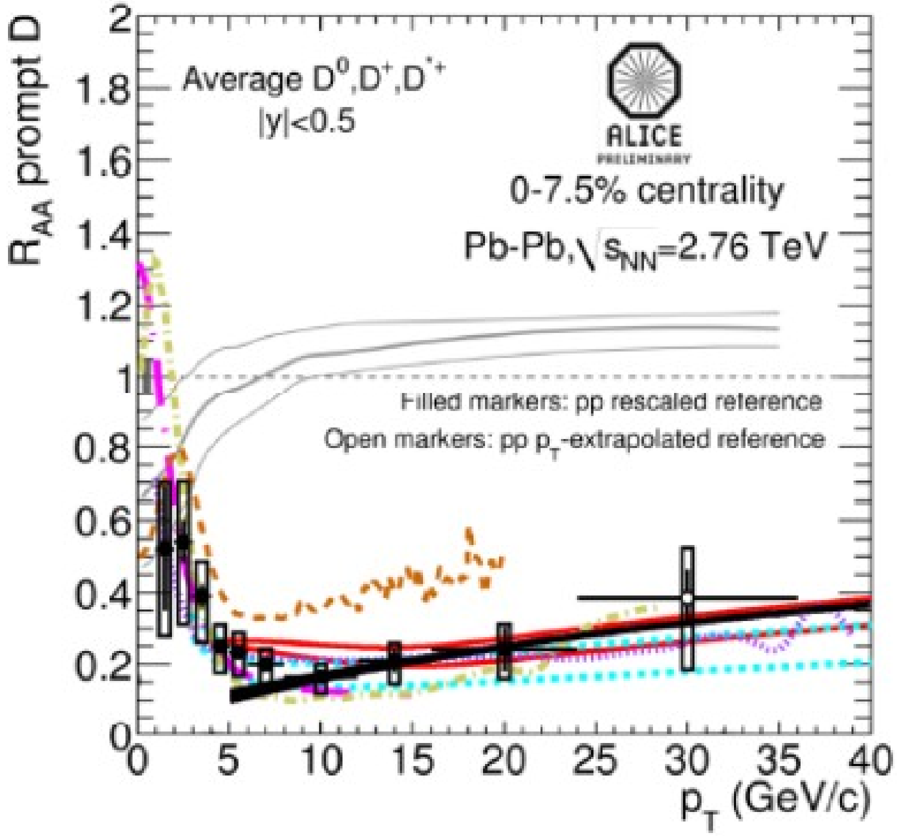

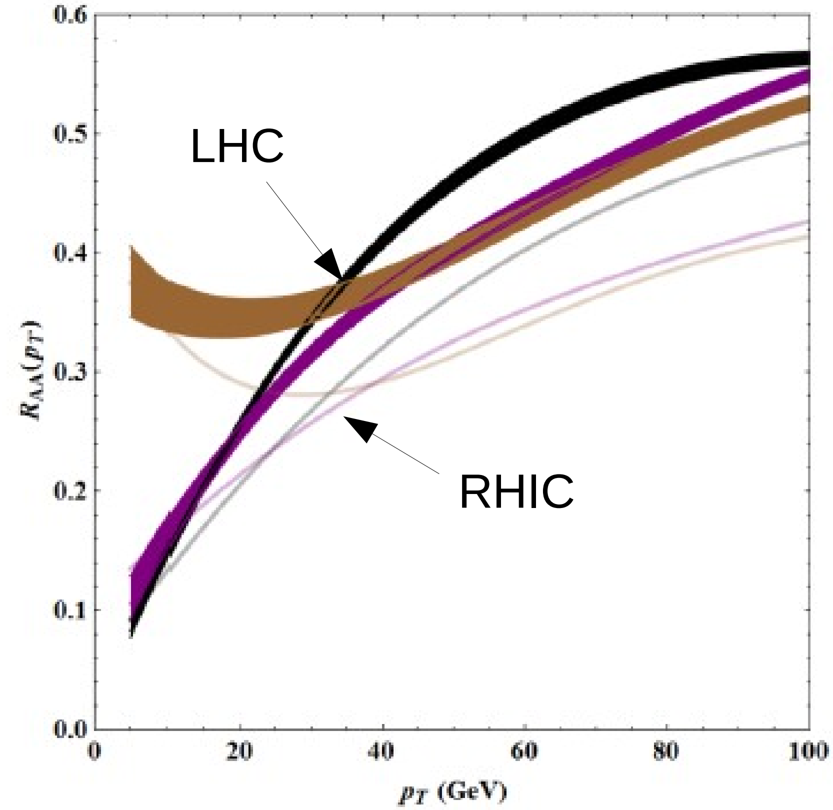

Figure 2: (Left) D meson R_{AA} at LHC. In black the running coupling CUJET results, constrained by the Pion fit shown in Fig. 1. Central 0% – 7.5% preliminary ALICE LHC data [9] are compared to predictions. (Right) Illustration of jet flavor tomography level crossing pattern of central R_{AA} versus p_T for Pions, D and B mesons. LHC Pb+Pb predictions are shown in solid color, RHIC Au+Au results are shown in faded colors. The opacity is constrained at LHC, given $dN/dy(LHC) = 2200$, by a fit to a reference point $R^{\pi}_{AuAu}(p_T = 40\text{ GeV}) = 0.35$ setting $\alpha_0 = 0.4$.

PQCD based DGLV naturally explains why RAA(D) ~RAA(pi)
But predicts a crossover B/D >1 pT<30 and B/D ~ 1 for pT >30
at both RHIC and LHC

G.Roland QM12: First evidence for B quark quenching

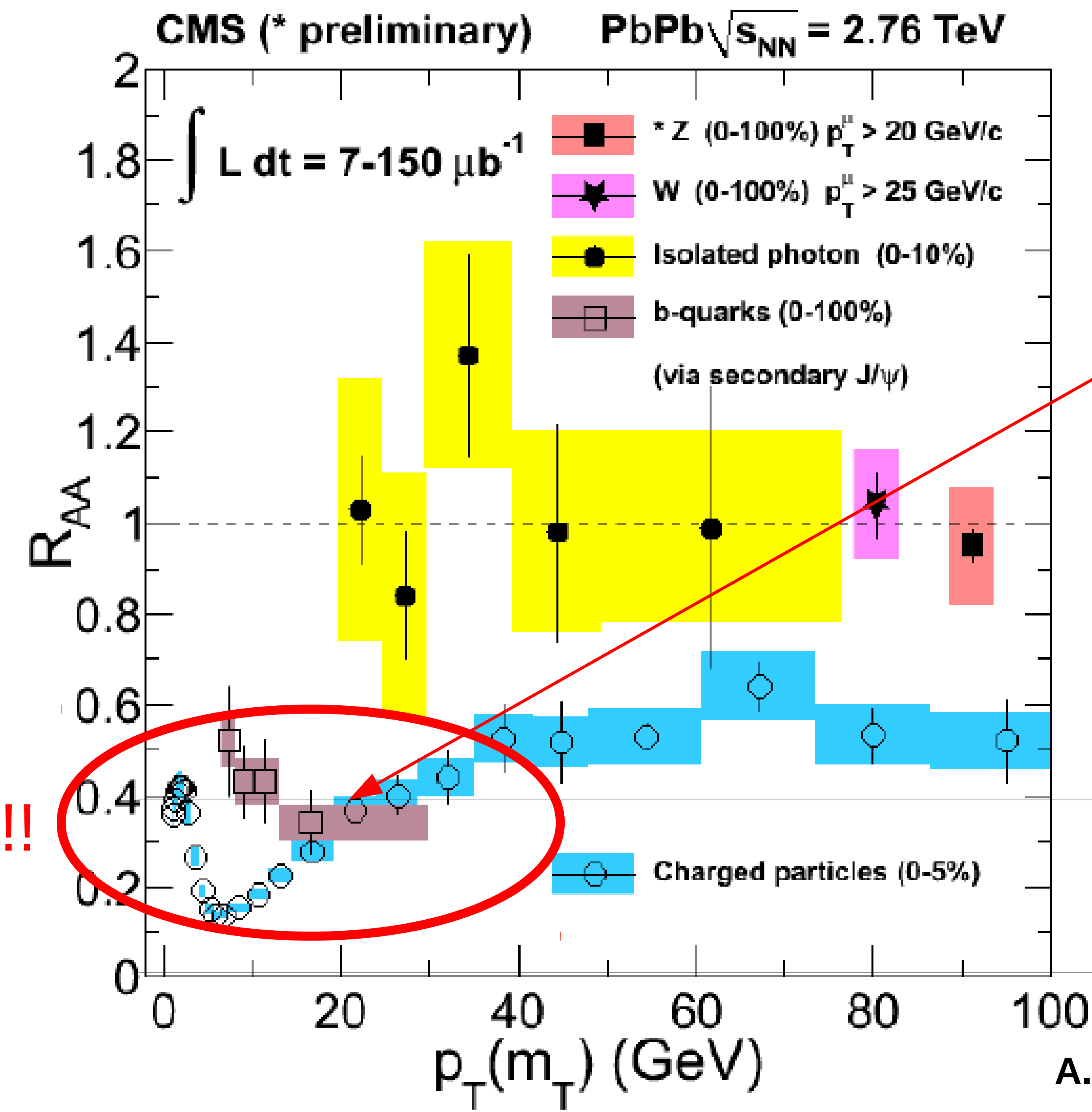

Has CMS seen
A hint of our predicted
RAA "Level Crossing"
Of B and pion RAA
??

CUJET1.0

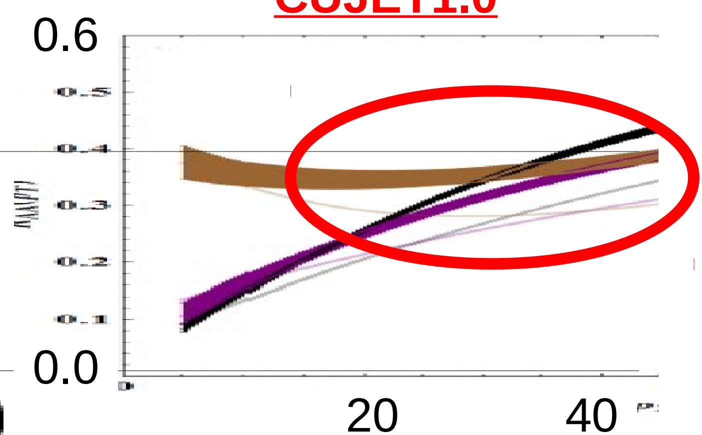

A. Buzzatti, MG, PRL 108 (2012)

Part 3: Our Jet v2 Albatross

The PHENIX v2 challenge to pQCD based Tomography

PHENIX A. Adare et al., arXiv:1208.2254

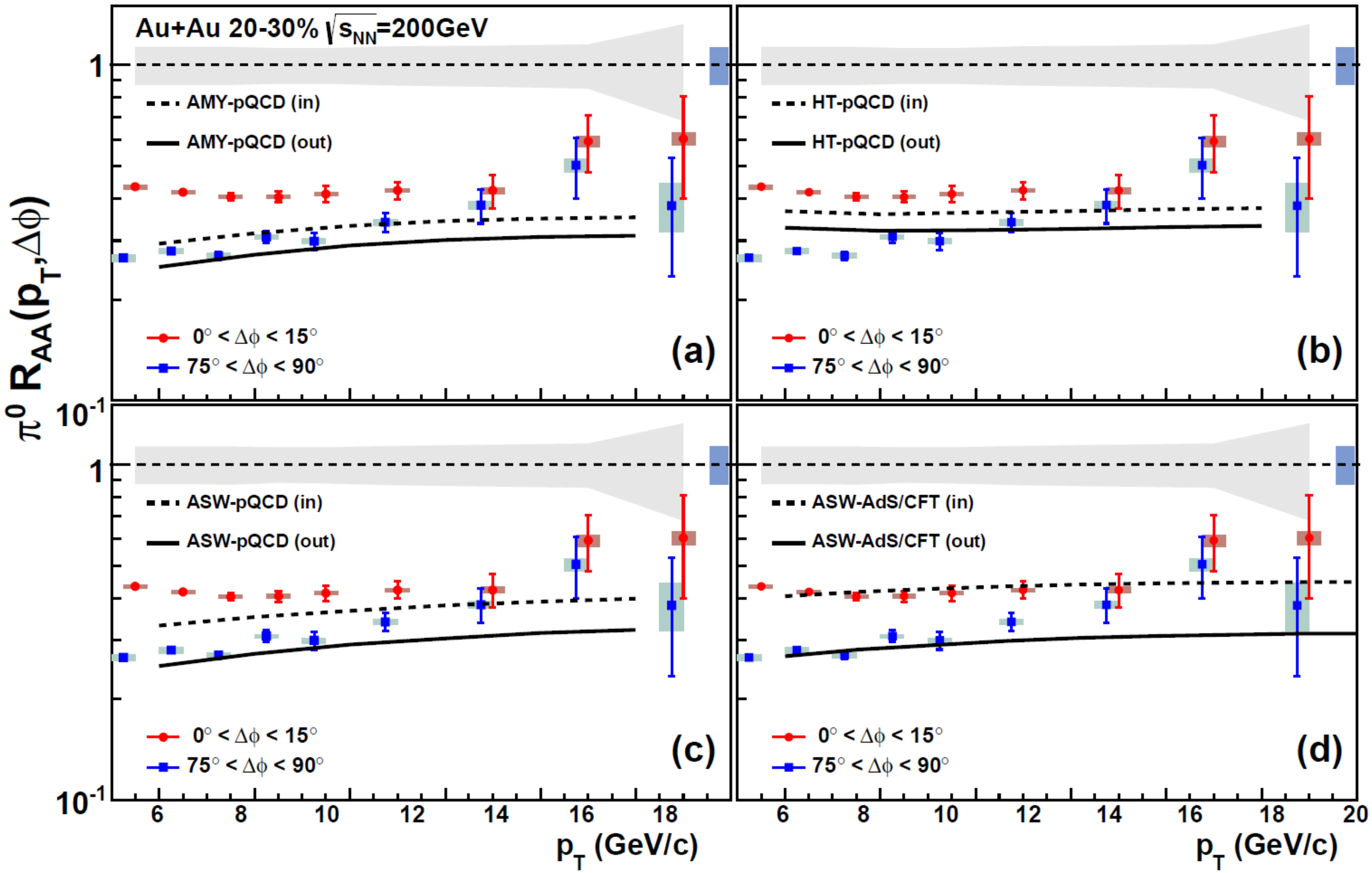

→ PHENIX claimed that only AdS/CFT like dE/dx= $\kappa\, x^2 T^4$ can fit R^{in}_{AA} and R^{out}_{AA} for (2+1)d transverse + Bj expanding QGP@RHIC

→ $R^{in}_{AA} = R_{AA}(1+2v_2)$ and $R^{out}_{AA} = R_{AA}(1-2v_2)$ provide information about *both* R_{AA} and v_2

Azimuthal Jet Tomography of Quark Gluon Plasmas at RHIC and LHC

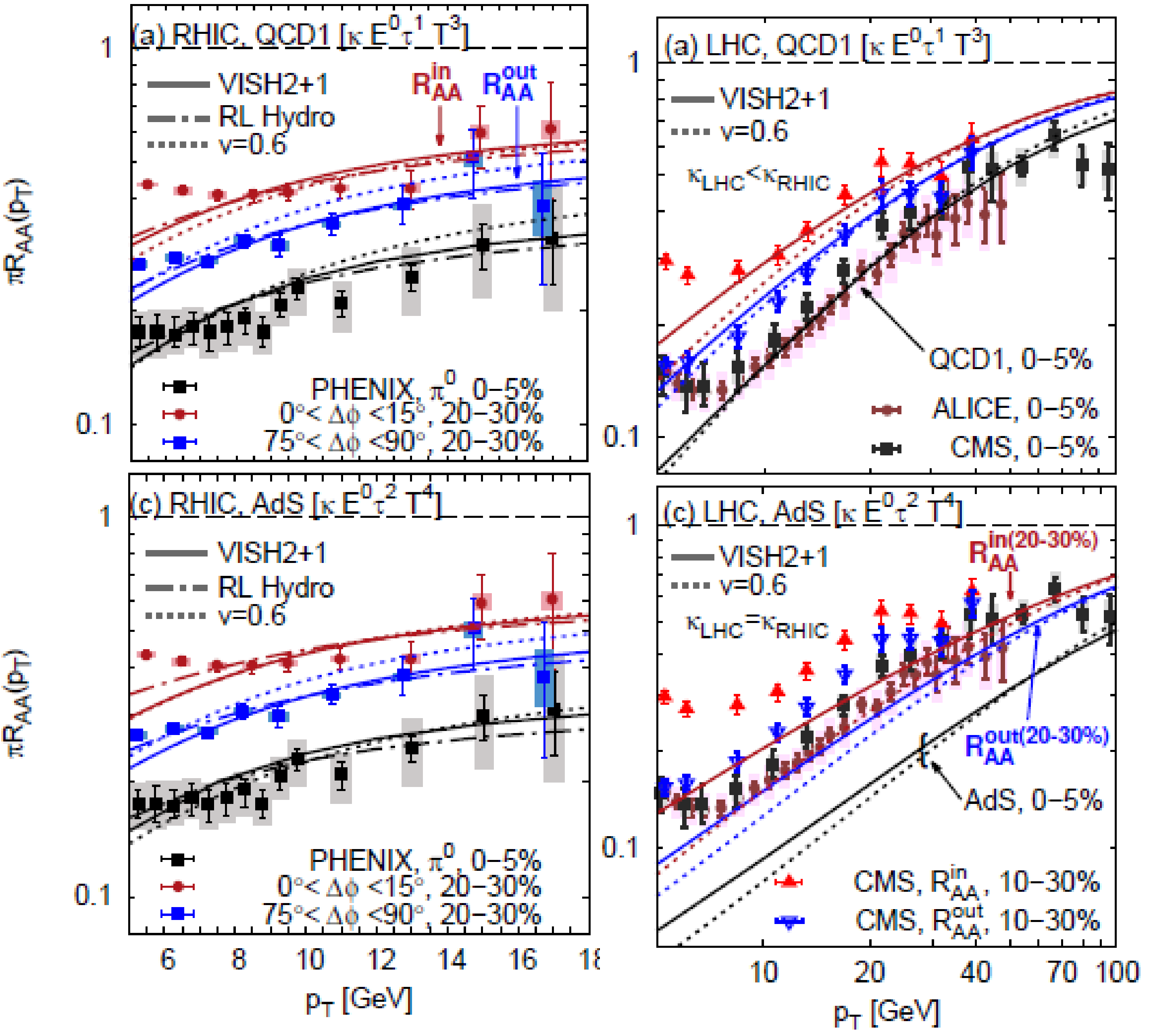

B.Betz, MG
arXiv:1305.6458
[nucl-th]

QCD1 ~ rc DGLV

“AdS” ~ fixed t'Hooft
conformal Falling Strings

Blast wave= GVWH 02

VISH2+1, Shen,Heinz,Song

RL-Romatschke,Luzum

RHIC Reference point
PT=7.5 , Central 5%
Raa= 0.2 for all models

RHIC and LHC data require reduction of jet-medium coupling at LHC as per pQCD
And hence rule out Conformal AdS Falling Strings and fcSL models.
We also contradict PHENIX's conclusion. [So our paper was rejected]

What makes jet v2(pT) difficult to compute?

B. Betz, MG 2013

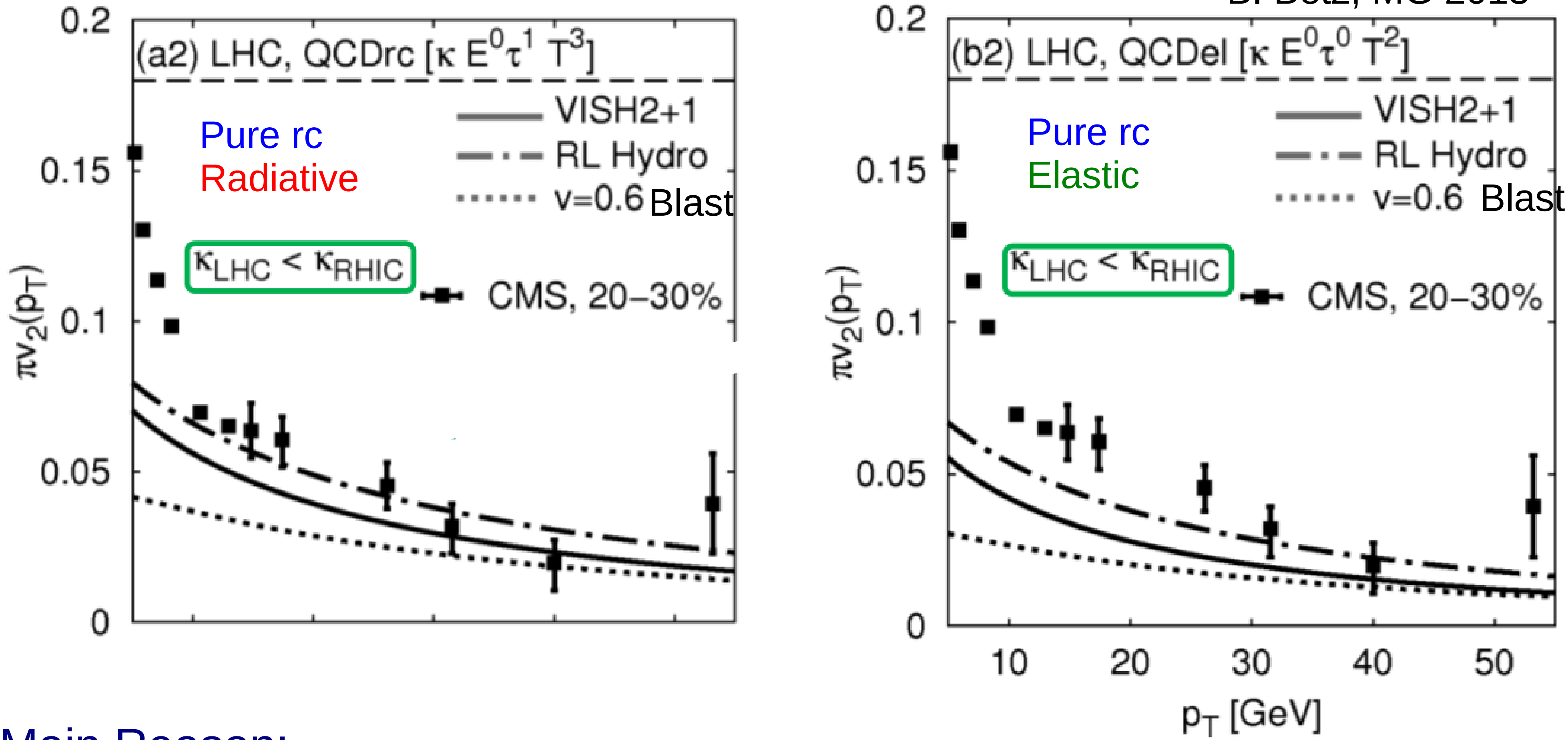

Main Reason:

v2 Jet ≈ ½ (dE/dx Model) + ½ (spacetime bulk hydro 2+1D flow) ← [“T.Renk's Lemma”]

Depends on the complex interplay between all details of microscopic pT>10 jet dE/dx
And all details of the spacetime evolution of the bulk soft pT<2 GeV sQGP (I.C., η/s, t_π)

Azimuthal averaged RAA is much less sensitive to this Hard+Soft convolution

Truth in Lending Act disclosure: CUJET2.0 's current v2 Albatross obeys Renk's Lemma

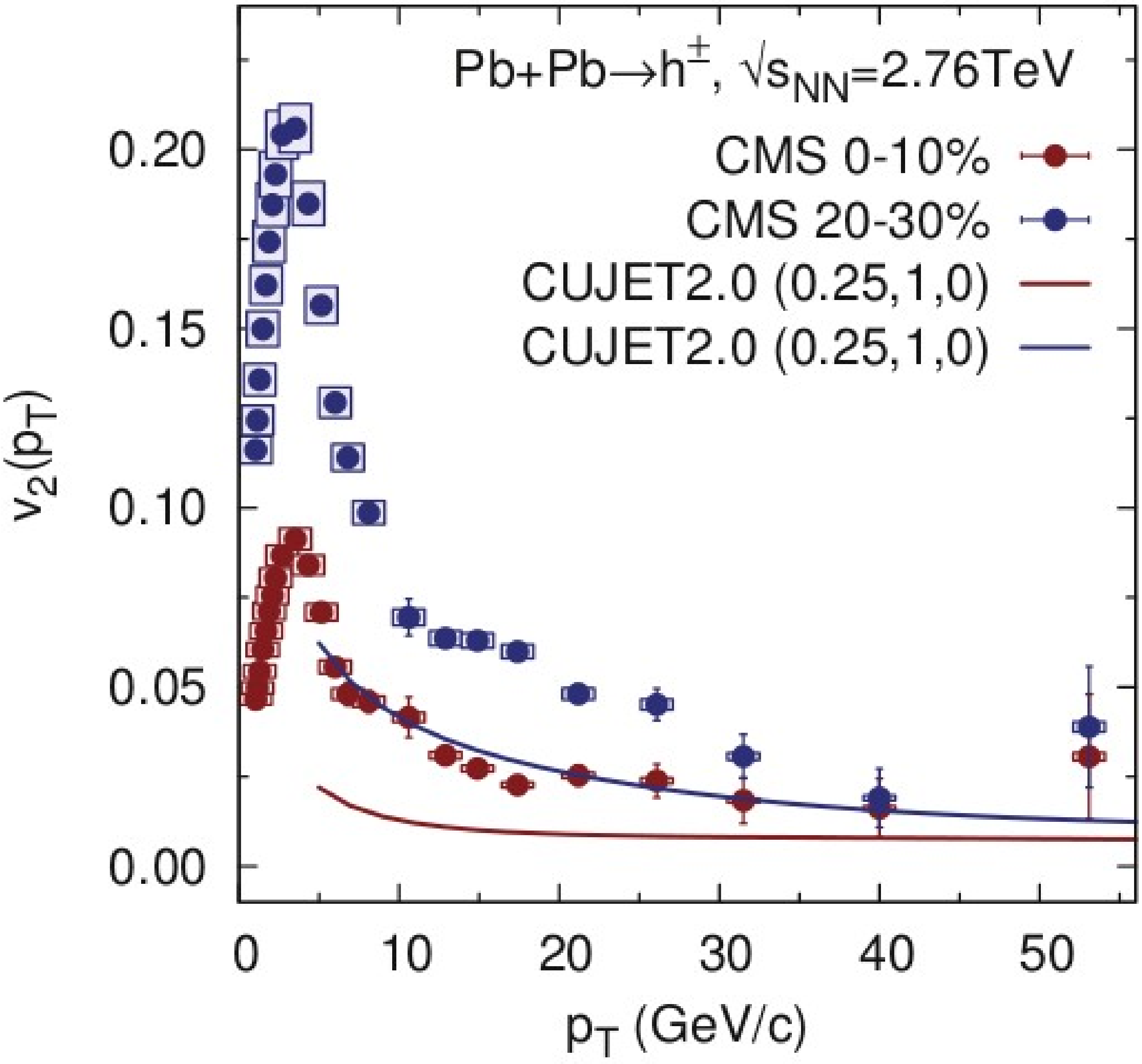

Part 4: CUJET2.0 = rcDGLV+VISH at RHIC and LHC and Constraints on the qhat(E,T) transport field

At first order in opacity

running coupling rcDGLV induced gluon radiative distribution is given by [62]

$$x\frac{dN_{Q->Q+g}}{dx}(\mathbf{x},\phi) = \int d\tau \rho_{QGP}(\mathbf{x}+\hat{\mathbf{n}}(\phi)\tau,\tau)\int \frac{d^2\mathbf{q}}{\pi}\frac{\alpha_s^2(\mathbf{q}^2)}{(\mathbf{q}^2+f_E^2\mu^2(\tau))(\mathbf{q}^2+f_M^2\mu^2(\tau))}\int\frac{d^2\mathbf{k}}{\pi}\alpha_s(k_T^2/(x(1-x))$$
$$\times\frac{12(\mathbf{k}+\mathbf{q})}{(\mathbf{k}+\mathbf{q})^2+\chi(\tau)}\cdot\left(\frac{(\mathbf{k}+\mathbf{q})}{(\mathbf{k}+\mathbf{q})^2+\chi(\tau)}-\frac{\mathbf{k}}{\mathbf{k}^2+\chi(\tau)}\right)\left(1-\cos\left[\frac{(\mathbf{k}+\mathbf{q})^2+\chi(\tau)}{2x_+E}\tau\right]\right).$$

where $\mu^2(\tau) = 4\pi\alpha_s(4T^2)$ is the local HTL color electric Debye screening mass squared in a pure gluonic plasma with local temperature $T(\tau) \propto \rho_{QGP}^{1/3}(\mathbf{x},\tau)$ along the jet path $\mathbf{x}(\tau)$ through the plasma. Here $\chi(\tau) = M^2x_+^2 + f_E^2\mu^2(T(\tau))(1-x_+)/\sqrt{2}$ controls the "dead cone" and LPM destructive interference effects due to both the finite quark current mass M, and a thermal gluon $m_g = f_E\,\mu(T)/\sqrt{2}$ mass.

We use the HTL deformation parameters (f_E, f_M) to vary the electric and magnetic screening scales relative to HTL= (f_E=1, f_M=0)

$\alpha_s(Q^2) = \min[\alpha_{max}, 2\pi/9\log(Q^2/\Lambda^2)]$ characterized by a nonperturbative maximum value α_{max}. The parameters (α_{max}, f_E, f_M) are therefore our main model control parameters.

CUJET2.0 couples rcDGLV to Bj + 2D transverse expanding QGP fluid fields (T(x,t),v(x,t))

One of many Bulk Hydro Examples :

- **VISH2 + 1 with eta = 0.08 ideal fluid results for RHIC b = 7 fm**

U.Heinz et al

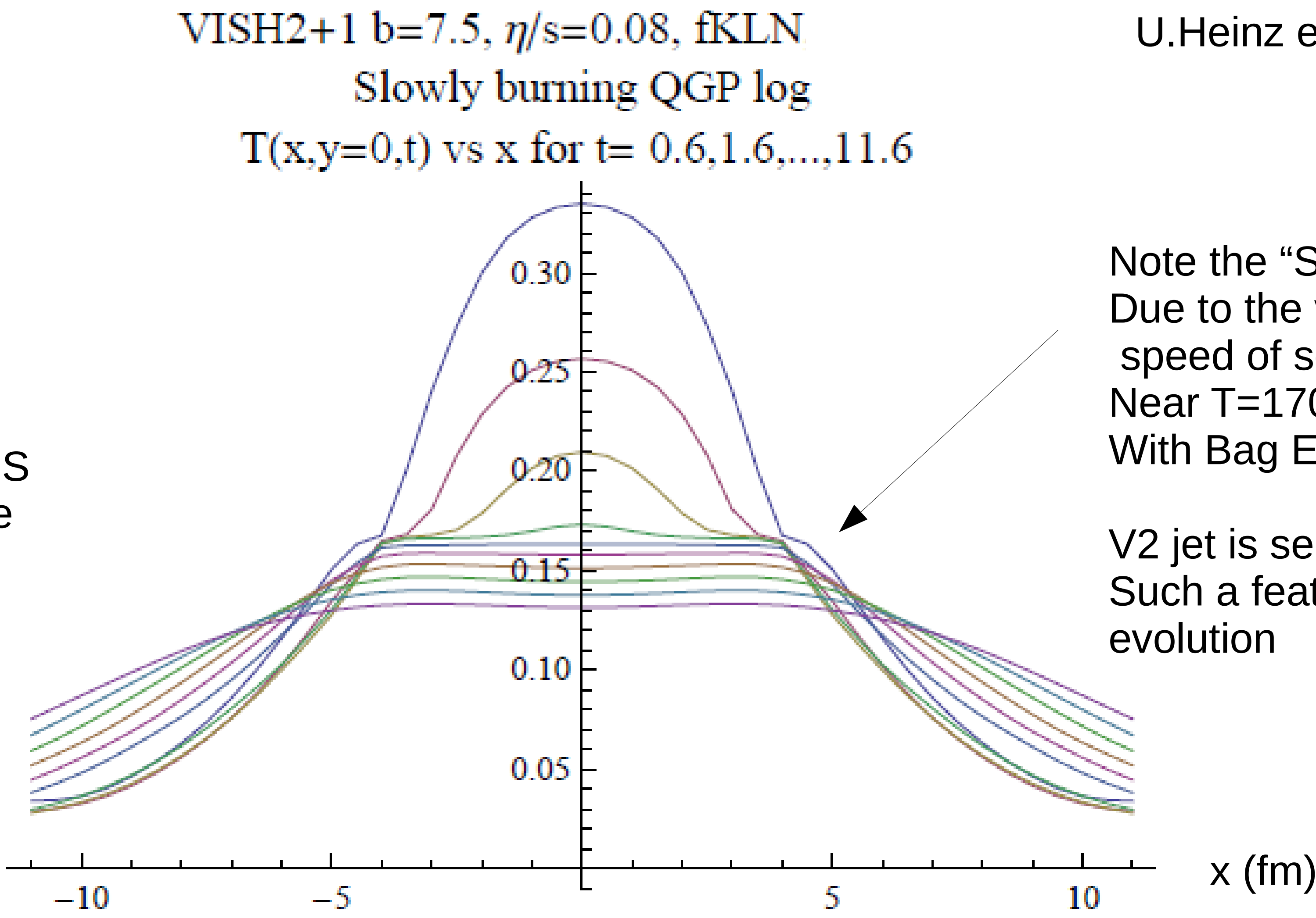

Bag EOS example

Note the "Stall"
Due to the vanishing speed of sound
Near T=170 MeV
With Bag EOS

V2 jet is sensitive to Such a feature of evolution

Note: Romatschke Luzum (RL) viscous hydro Thermal field evolution differ in detail

J.Xu, MG prelim

Consistency of CUJET2.0 with RHIC vs LHC central RAA vs alpha_max (running coupling saturation parameter) (in HTL fE=1, fB=0 approx in VISH2.1 hydro fields)

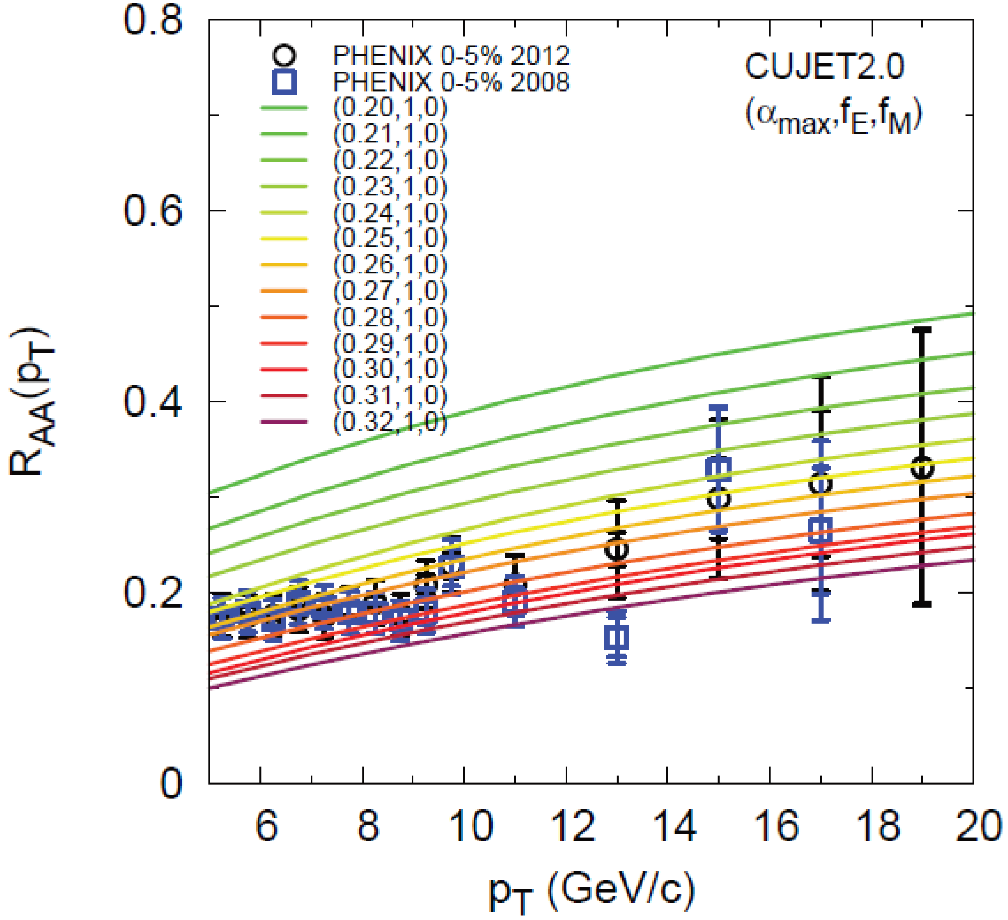

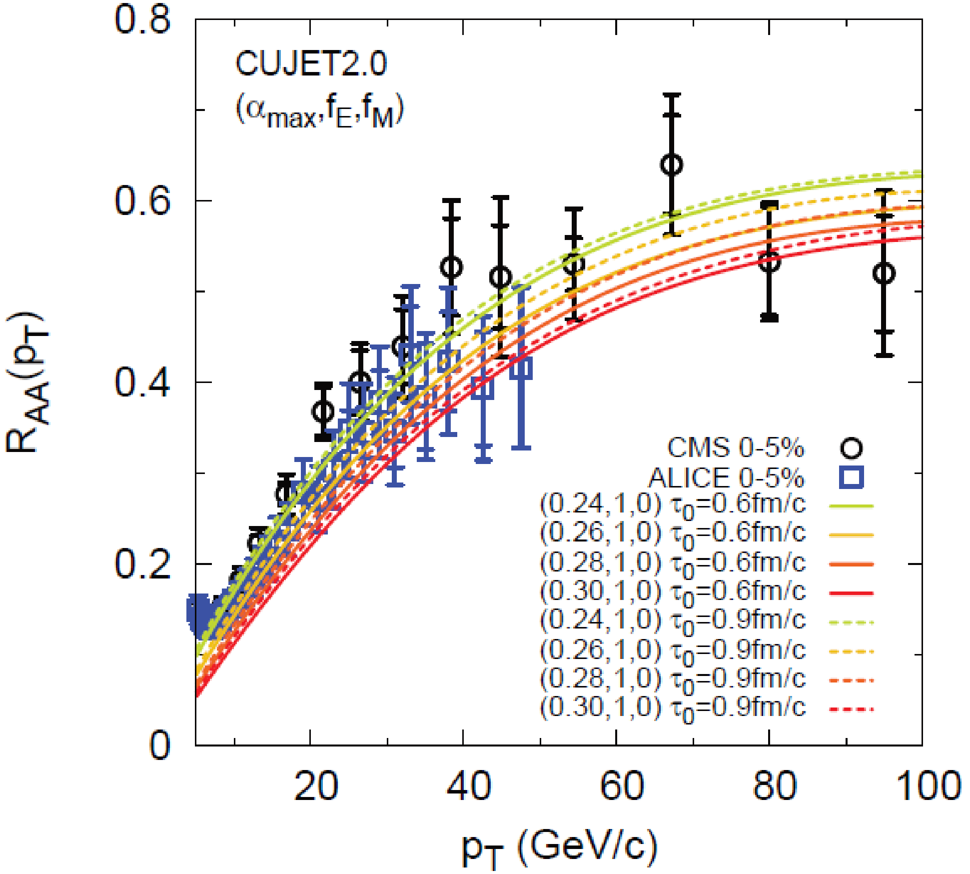

Chi-Squared(pT>8 GeV) of CUJET2.0 vs α_{max} using RHIC and LHC central RAA charged (for HTL fE=1, fM=0 , VISH2+1)

$\alpha_{max} = 0.26 \pm 0.01$

J,Xu, MG prelim

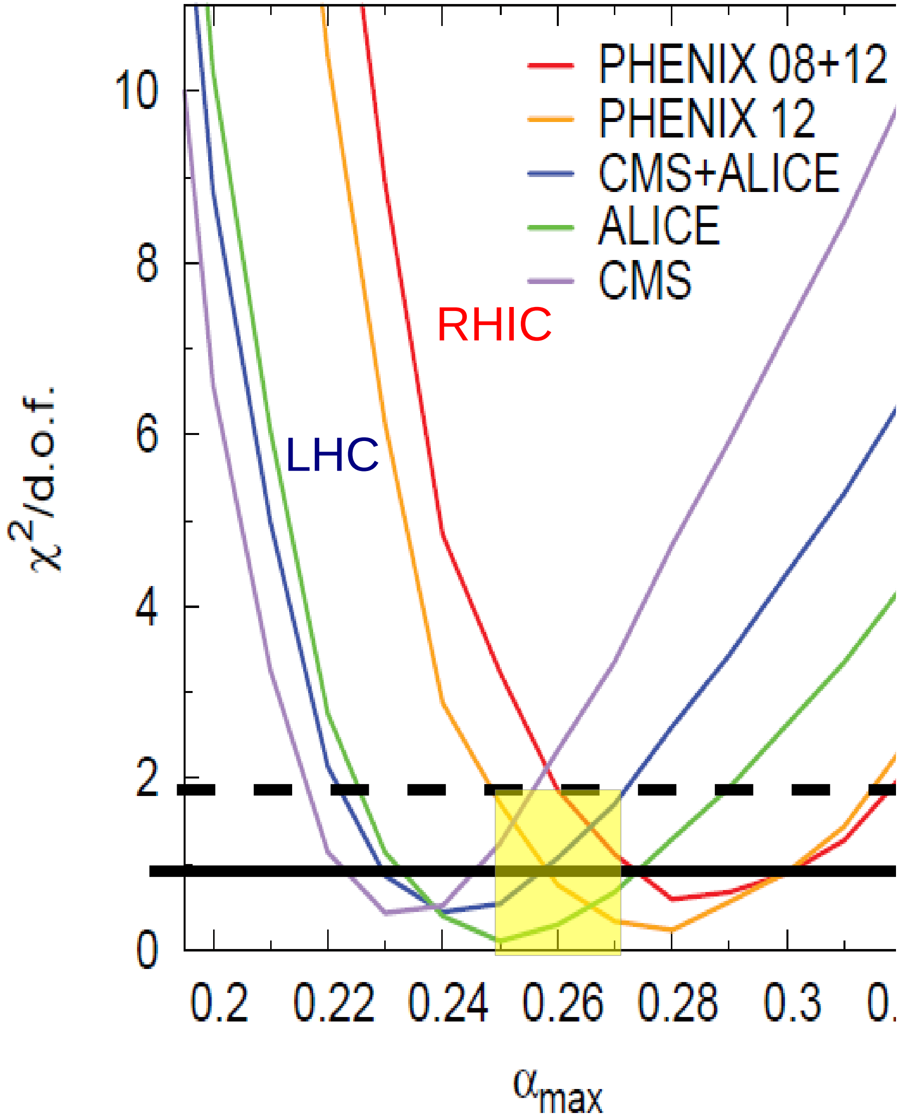

RHIC combined vs **LHC combined**

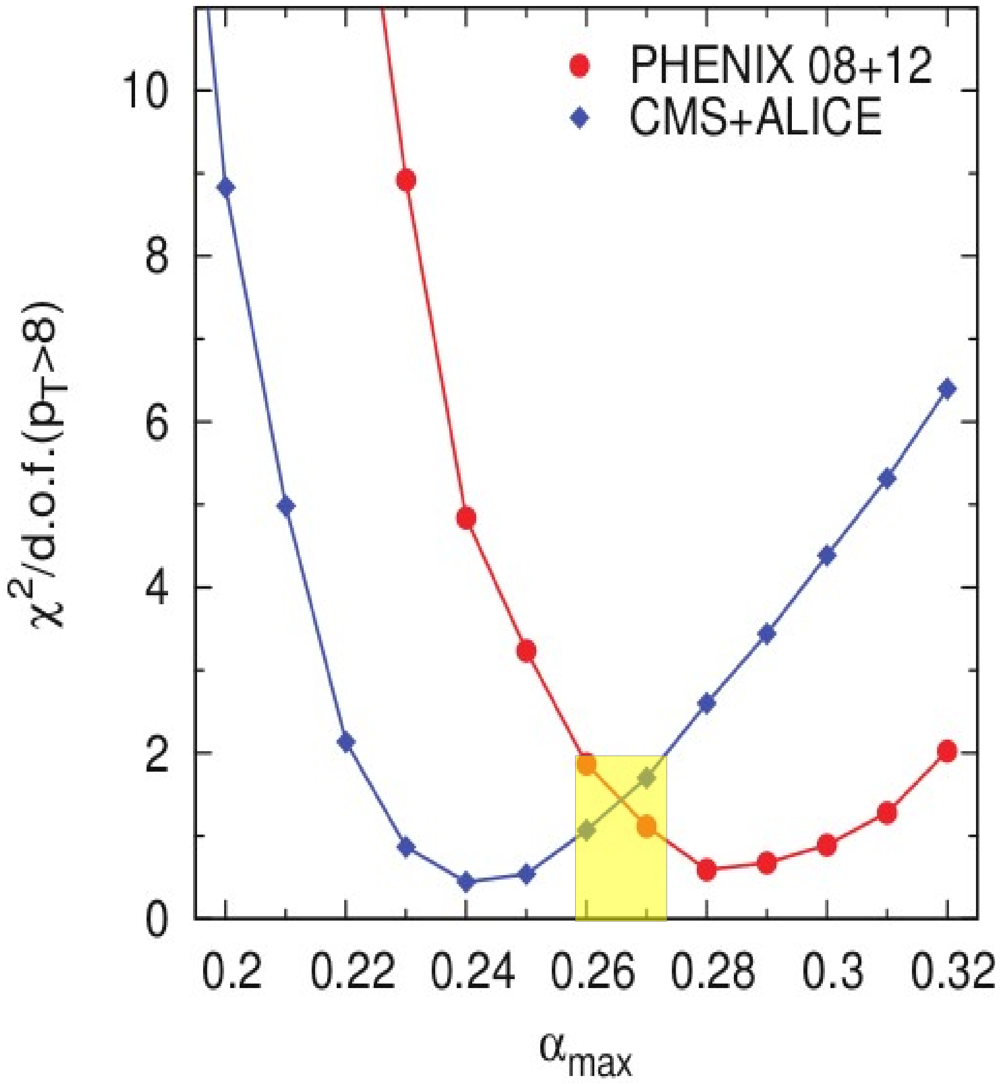

Likelihood analysis of HTL mu ~ g T vs Lattice-like mu ~ 2 g T

Surprisingly RHIC+LHC data prefer HTL mu ~ gT **J.Xu, MG prelim**

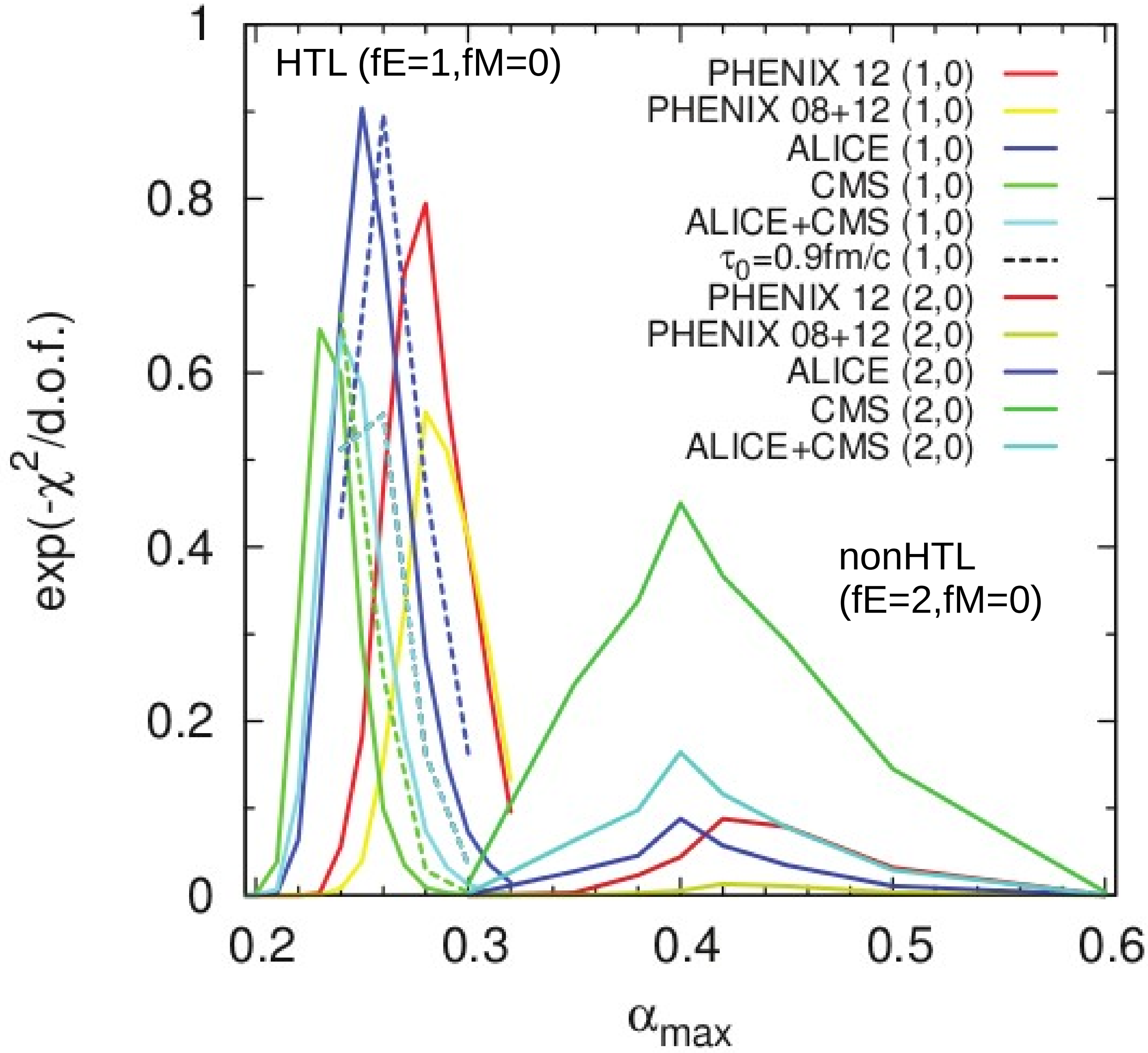

J.Xu, MG prelim

CUJET2.0 RHIC + LHC constrained qhat(T,E) *field*

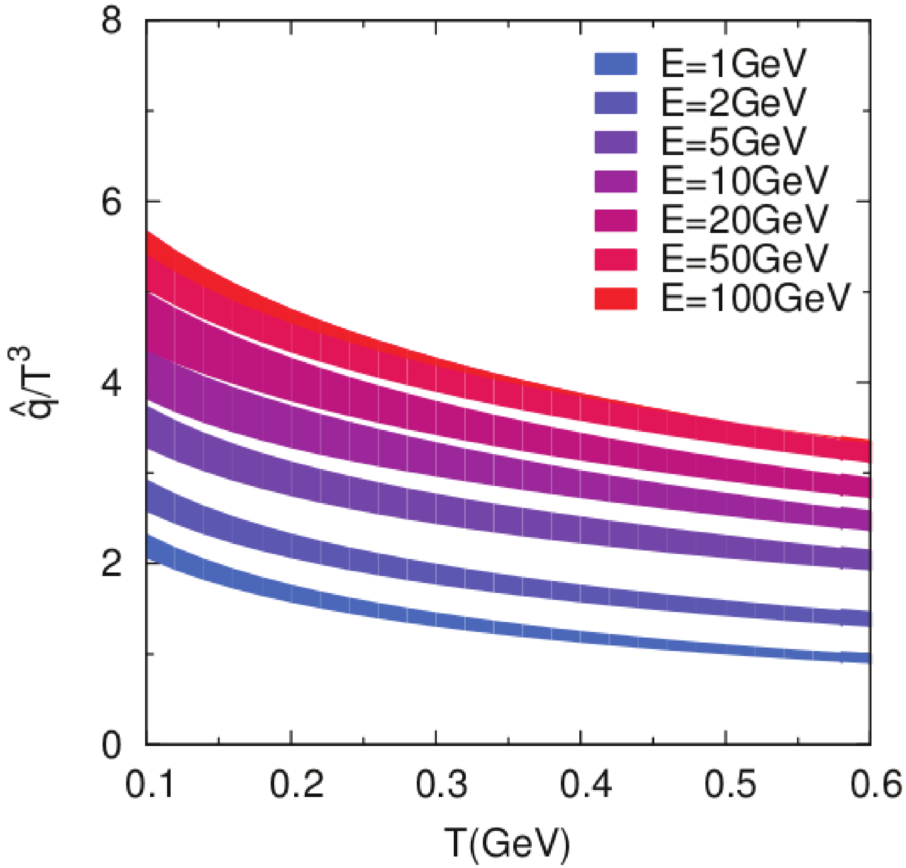

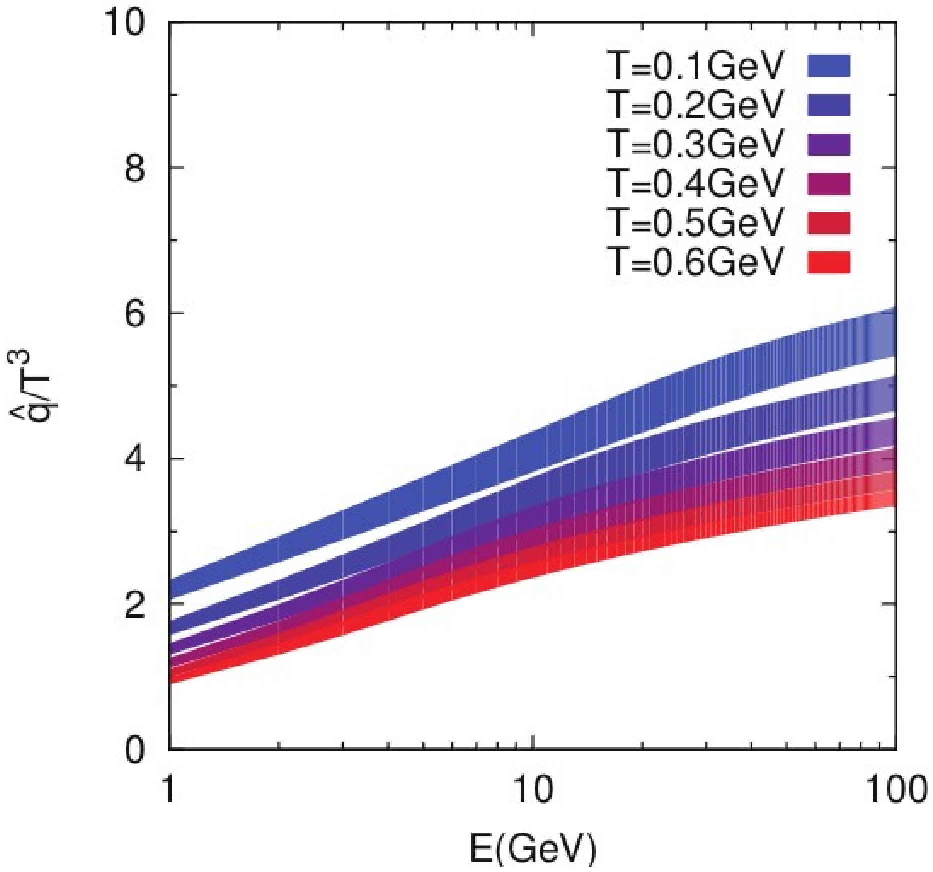

Comparison of JET Collab's present results qhat(T,E)

X.N.Wang et al

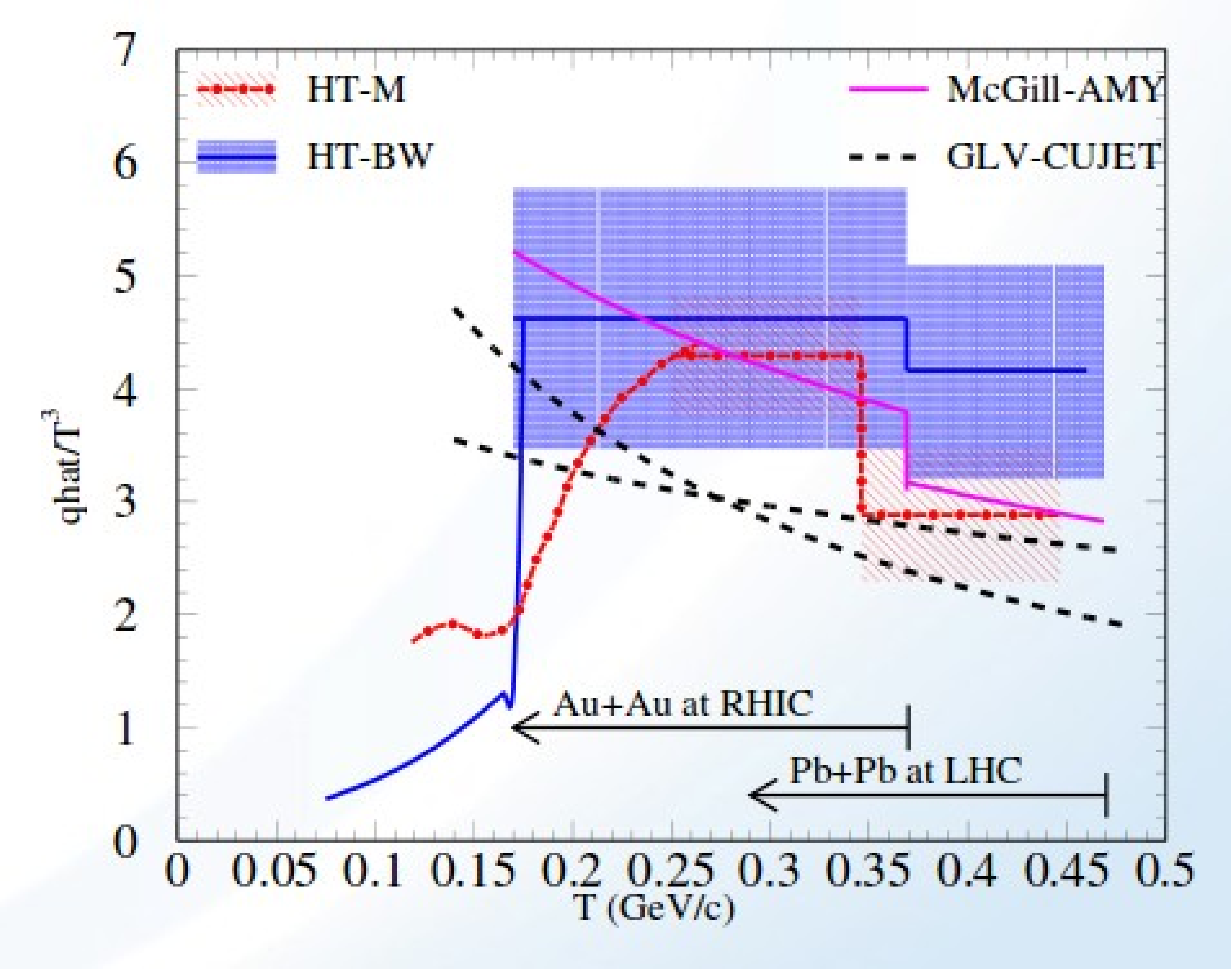

CUJET2.0 compatibility with single e @ RHIC and D @ LHC

J,Xu, MG prelim

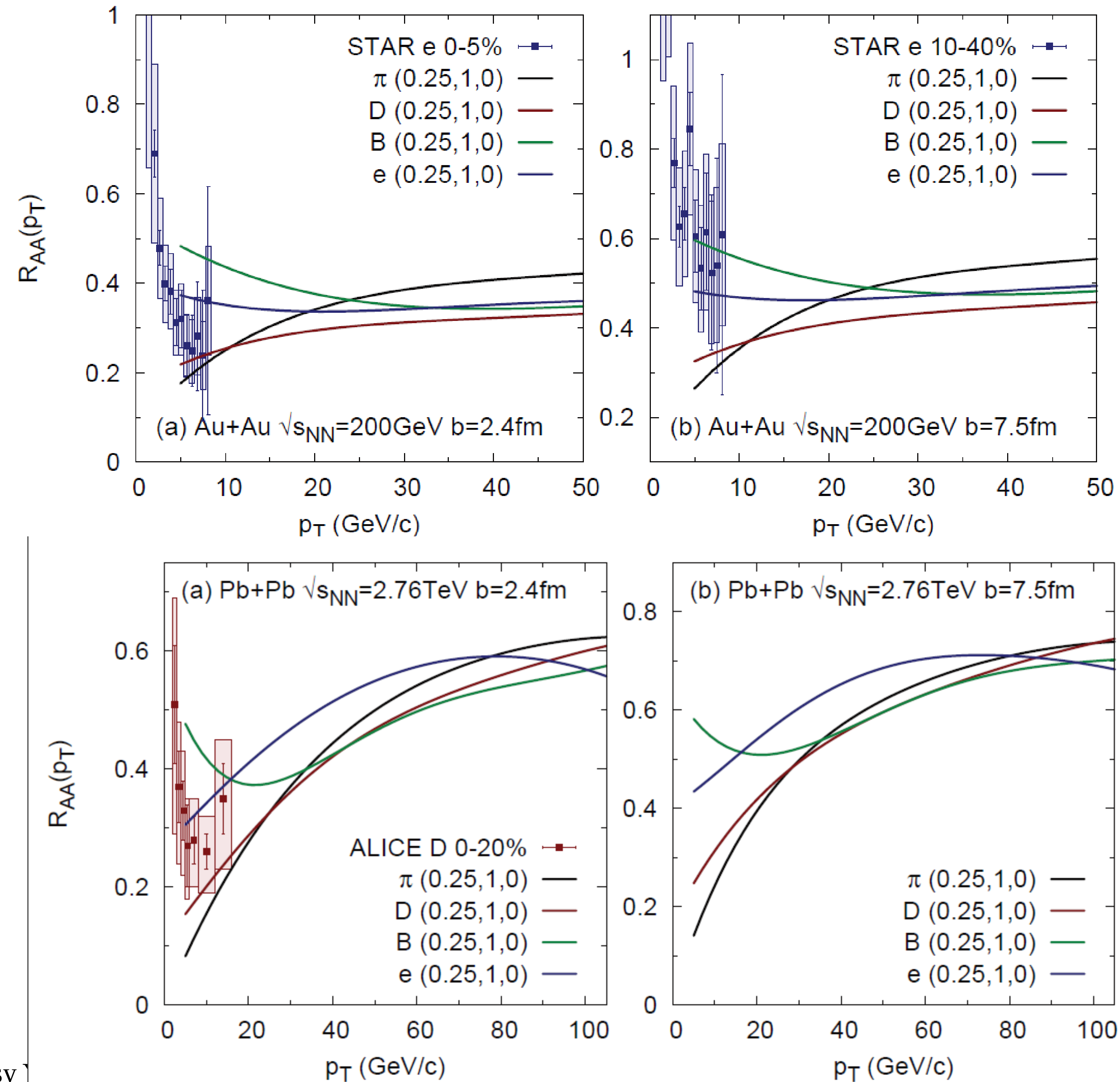

The AdS/CFT conjecture:

Maldacena, Witten
Klebanove, Gubser ...

- 4D $\mathcal{N} = 4$ supersymm quantum Yang Mills $\equiv$ 4D Minkowsky "boundary" of classical supergravity+string in a 10D $AdS_5 \times S^5$ spacetime

- Duality holds strictly only in the "'t Hooft limit":

$$N_c \gg \lambda \gg 1 \qquad \lambda = g_{YM}^2 N \sim 6$$

- **Is 3 >> 6 >>1 ??** (for $\alpha_s \sim 0.3$ << 1 ??)

- 1/Nc corrections via Gauss Bonnet R^2 action can account for <u>less than perfect</u> QGP fluids with $\eta/s > 1/4\pi$

- Dilaton-AdS-BH deformations of metric can account for <u>non-conformal</u> lattice QCD thermo data

- Jet-QGP interactions are encoded in the classical string-metric action

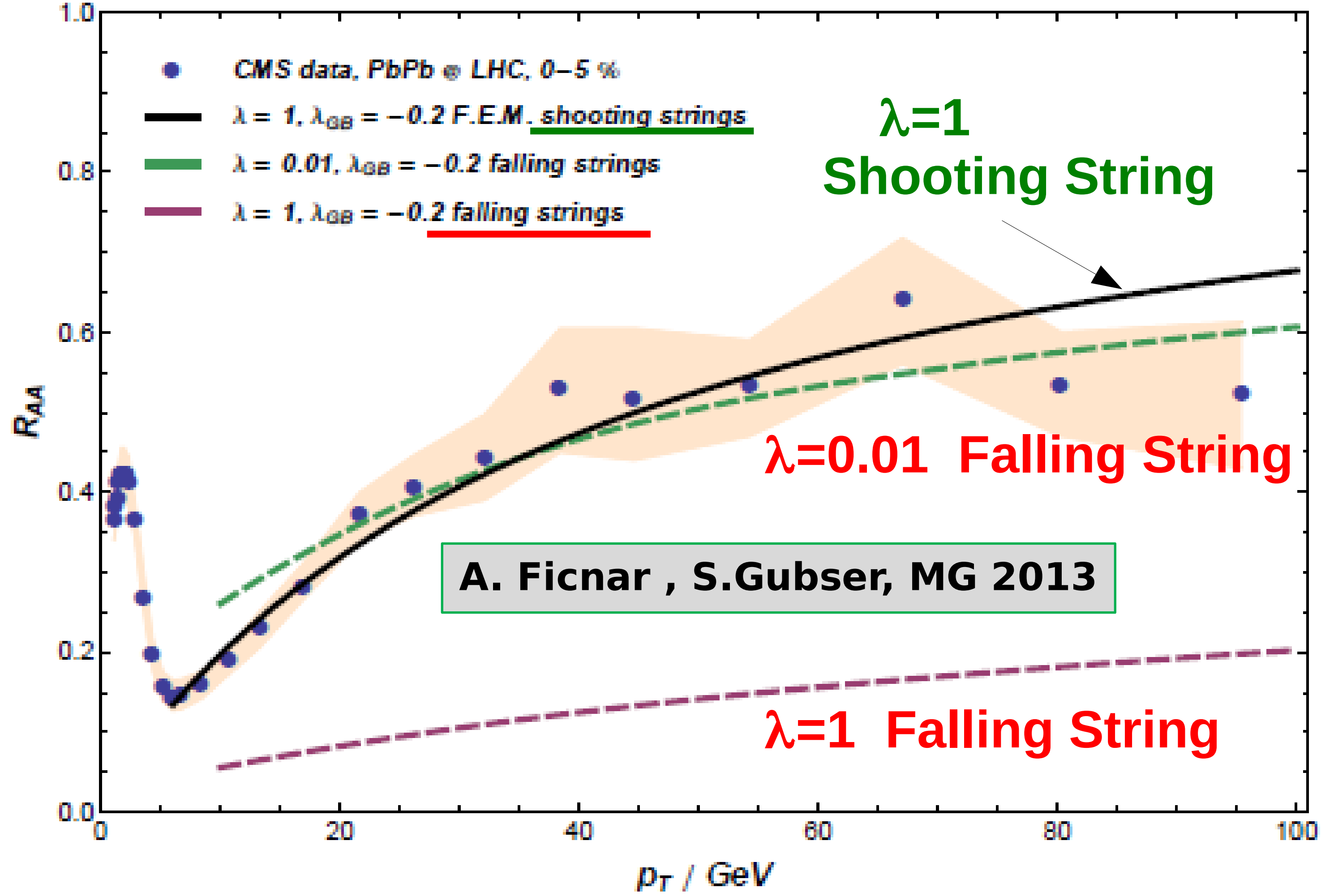

FIG. 1. Model calculations of the nuclear suppression factor R_{AA} of pions in central collisions at the LHC, compared to the CMS data [7]. Dashed lines are the calculations from [6], done using the energy loss inferred from the falling strings, and the solid line represents the R_{AA} computed in the framework of the finite endpoint momentum strings, which we describe in this Letter. All three curves were computed with the higher derivative Gauss-Bonnet corrections to AdS_5.

Summary:

Falling strings require unphysically small λ~ 0.01 to account for "Surprising Transparency" of QGP@LHC LHC

But Shooting String With λ=1 can explain LHC data

All curves include λGB = - 0.2 => η/s = 1.8 X(1 /4pi)

***<u>Half Perfect</u>* viscosity Needed by viscous Hydro to fit bulk v2 Using KLN/CGC IC**

(The QGP@RHIC is only Half Perfect)

Finite endpoint shooting strings:

A. Ficnar , S.Gubser, 2013

- Endpoint trajectories are null geodesics
- Maximum stopping distance is ~2.4X greater:

Start from z0=zH

$$\Delta x_{\rm stop} = \left[\frac{2}{\pi^{2/3}} \frac{\Gamma\left(\frac{5}{4}\right)\Gamma\left(\frac{1}{4}\right)^{1/3}}{\Gamma\left(\frac{3}{4}\right)^{4/3}} \right] \frac{1}{T}\left(\frac{E}{\sqrt{\lambda}T}\right)^{1/3} \sim 2.4 \ (\Delta x_{\rm stop})^{\rm falling}$$

1.248 shooting vs 0.526 falling strings =>

For fixed E, T, and Δx_{stop} > L

λ(shoot) ~ 200 X λ(fall) !

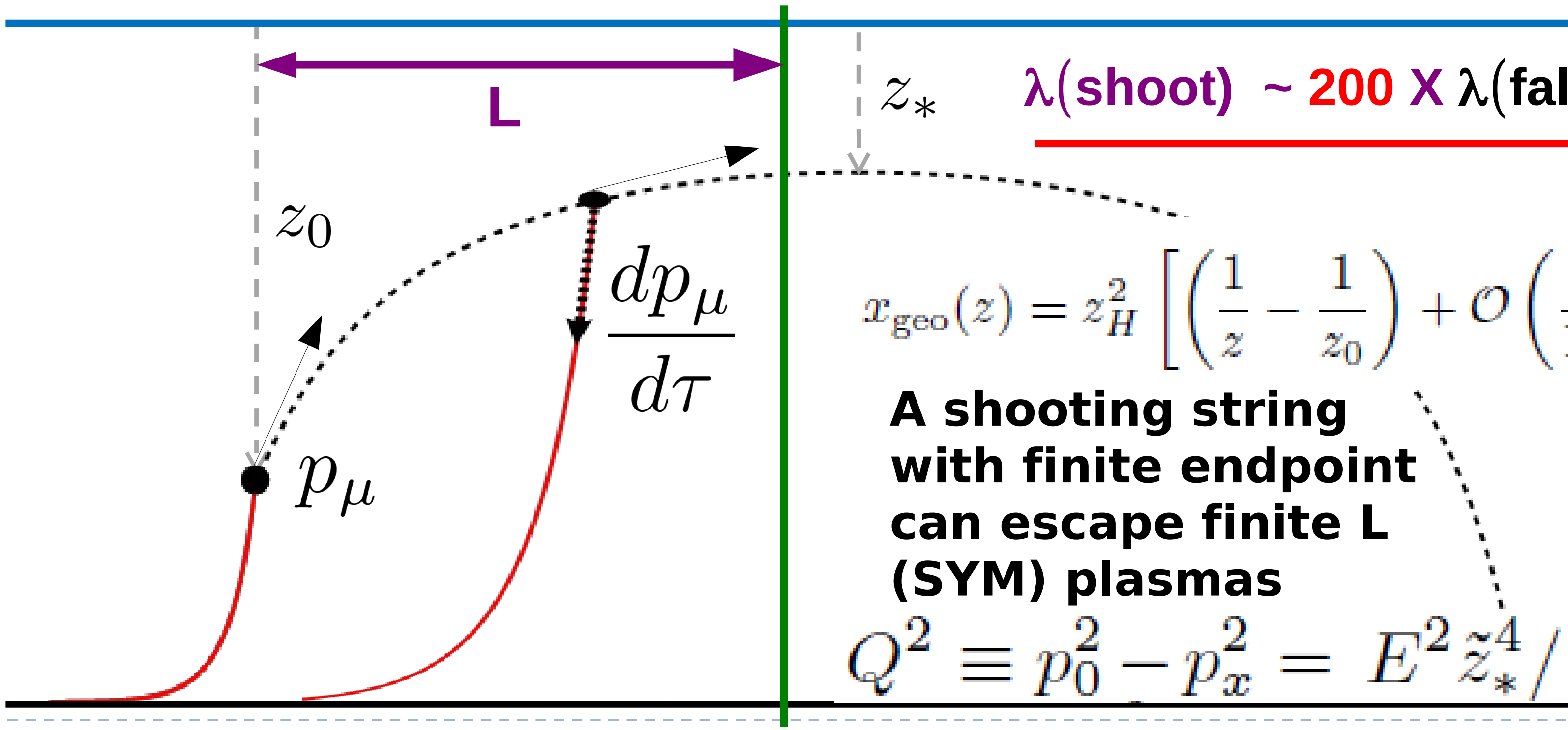

$$x_{\rm geo}(z) = z_H^2 \left[\left(\frac{1}{z} - \frac{1}{z_0}\right) + \mathcal{O}\left(\frac{z_*^4}{10 z^5}, \frac{z_*^4}{10 z_0^5}\right)\right.$$

A shooting string with finite endpoint can escape finite L (SYM) plasmas

$$Q^2 \equiv p_0^2 - p_x^2 = E^2 z_*^4 / (1 - z_*^4 / z_H^4)$$

A. Ficnar , S.Gubser, 2013

Finite momentum string endpointaction

- Introduce finite endpoint momentum via surface term:

$$S = -\frac{1}{4\pi\alpha'}\int_M d\tau d\sigma\,\sqrt{-h}h^{ab}\partial_a X^\mu \partial_b X^\nu G_{\mu\nu} \; + \int_{\partial M} d\xi\,\frac{1}{2\eta}\dot{X}^\mu \dot{X}^\nu G_{\mu\nu}$$

Nambu-Goto world sheet + a new boundary term

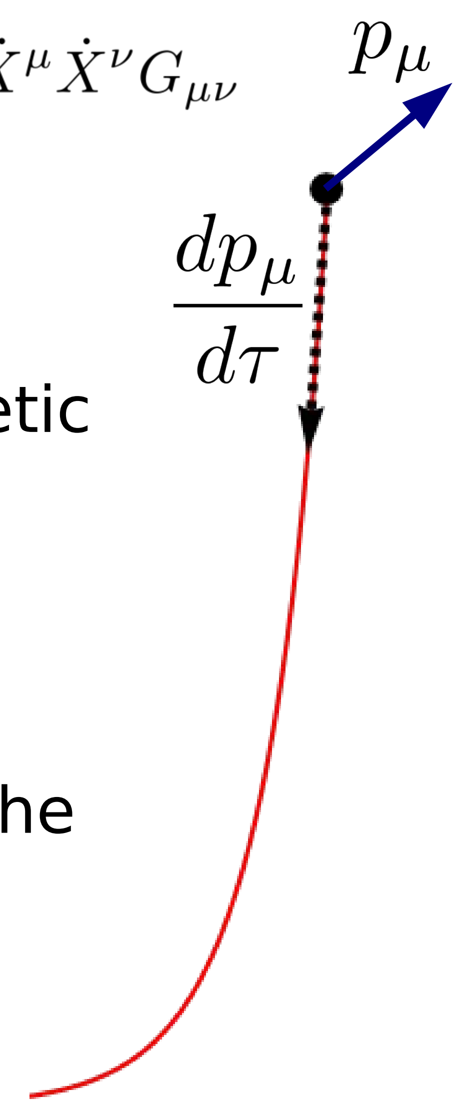

A more natural "Lund"like description of an energetic point quark and its color flux tube:

- Endpoint is the point quark,
- String = its nonlocal "color field"

- **Unique definition** of the jet energy loss from the endpoint into the bulk of the string

$$\dot{p}_\mu - \Gamma^\kappa_{\mu\lambda}\dot{X}^\lambda p_\kappa = \mp\frac{\eta}{2\pi\alpha'}p_\mu = \mp\frac{1}{2\pi\alpha'}G_{\mu\nu}\dot{X}^\nu$$

Finite endpoint momentum - energy los

- A universal form of the energy loss:

Ficnar, Gubser & Gyulassy, to appea

$$\frac{dE}{dx} = -\frac{\sqrt{\lambda}}{2\pi}\frac{\sqrt{f(z_*)}}{z^2} \qquad \sqrt{\lambda} = L^2/\alpha' \qquad f(z) = 1 - \frac{z^4}{z_H^4}$$

  - Local quantity, independent of initial conditions & bulk shape of string
  - Independent of energy stored in the endpoint (R_{AA} increases with p_T)

- Solve for (critical) null geodesics: z* → 0 $\quad \tilde{z}_0 \equiv \pi T z_0 \in [0,1]$

$$\frac{dE}{dx} = -\frac{\pi}{2}\sqrt{\lambda}T^2\left(\frac{1}{\tilde{z}_0} + \pi T x\right)^2$$

New Shooting string "pocket" formula Interpolates between pQCD and old AdS ansat

- $\sim T^2$ for small x — like pQCD collisional e-loss
- $\sim xT^3$ for intermediate x — like pQCD radiative e-loss (only path dep.)
- $\sim x^2T^4$ for large x — old "AdS" e-loss e.g. Marque Renk, 20

Even though now "reasonable" $\lambda = 3$ fits RHIC RAA
Shooting String Holography in a Conformal AdS bulk
cannot explain similarity of RHIC and LHC RAA

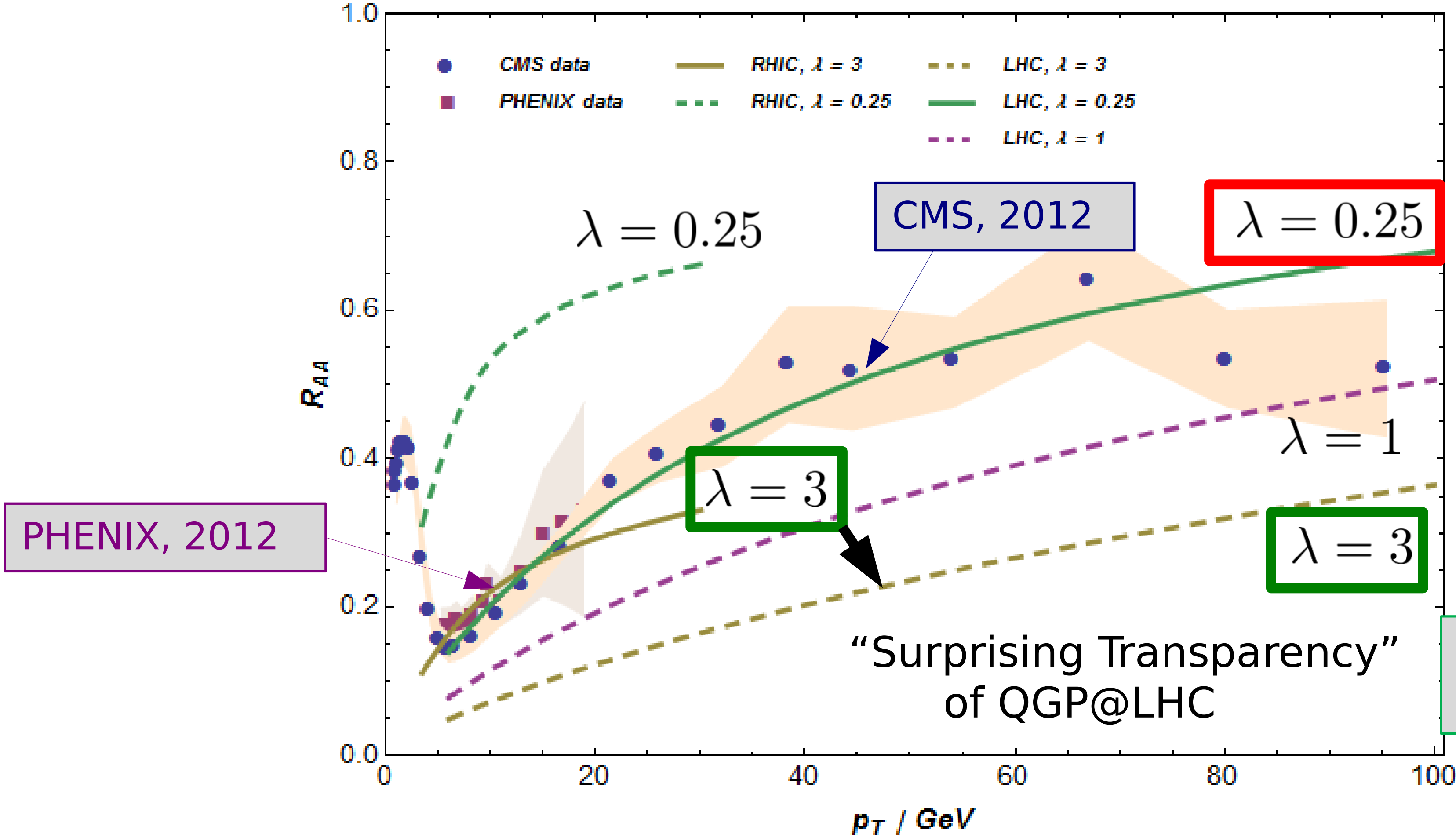

Similar RAA
ALICE data
Not shown

W.Horowitz, MG
WHDG 2011

Even though a more "reasonable" λ=3 now accounts for RHIC RAA
Shooting String Holography in Conformal AdS bulk
cannot explain the similarity of RHIC and LHC RAA
with same t'Hooft coupling !

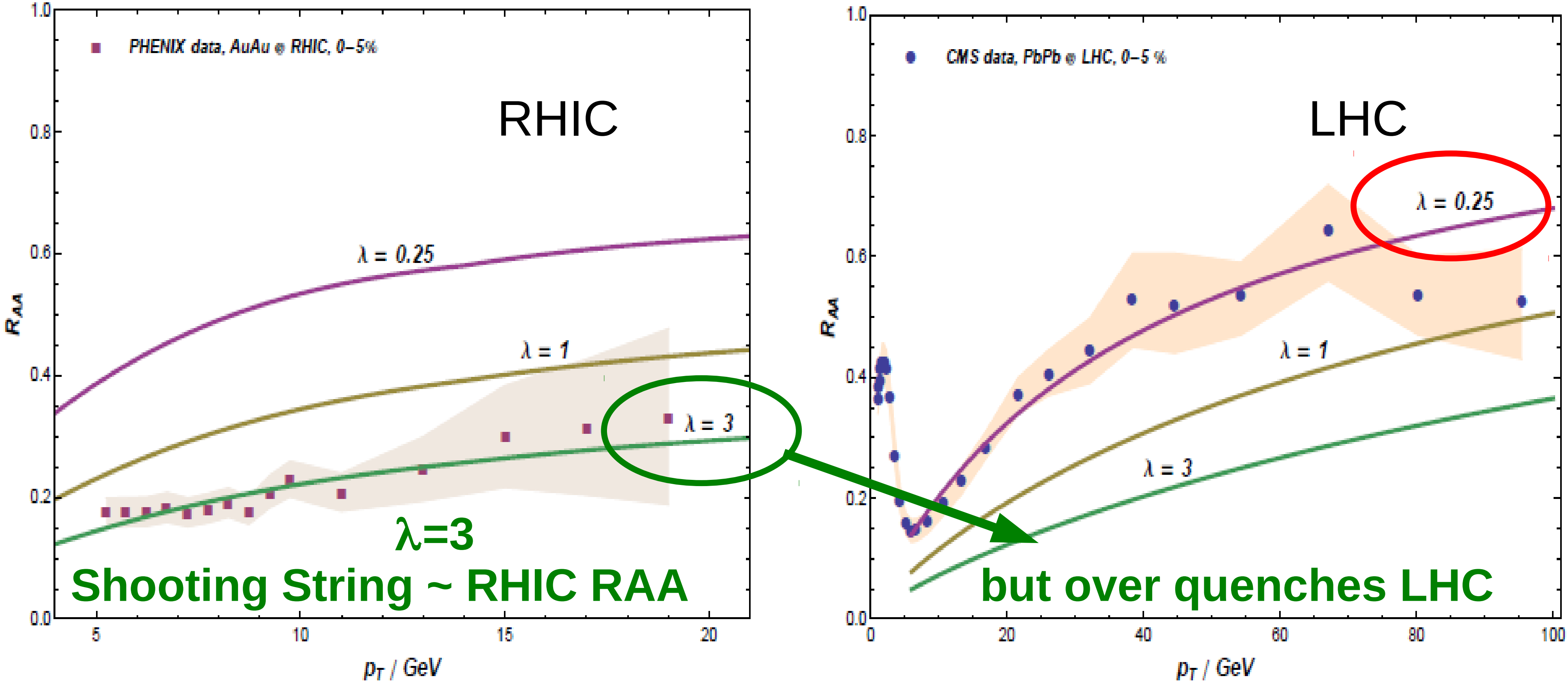

FIG. 2. Nuclear modification factor R_{AA} of pions in central collisions at RHIC and LHC. Our calculations are compared to the experimental data from the PHENIX [19] and the CMS [7] collaborations for 0-5 % centrality class. In different plots we only change the 't Hooft coupling λ while they all have the same impact factor of $b = 3$ fm, the freezout temperature of $T_{\text{freeze}} = 170$ MeV, the formation time of $t_i = 1$ fm/c and the initial $\tilde{z}_0 = 1$ (from (2.4)).

A. Ficnar , S.Gubser, MG 2013

We will model the R^2 corrections by a Gauss-Bonnet term, i.e. we will consider the action of the form:

$$S = \frac{1}{2\kappa_5^2}\int d^5x\sqrt{-G}\left[R + \frac{12}{L^2} + L^2\frac{\lambda_{GB}}{2}\left(R^2 - 4R_{\mu\nu}^2 + R_{\mu\nu\rho\sigma}^2\right)\right] \quad (4.1)$$

where λ_{GB} is a dimensionless parameter, constrained by causality [20] and positive-definiteness of the boundary energy density [21] to be:

$$-\frac{7}{36} < \lambda_{GB} \leq \frac{9}{100}\,. \quad (4.2)$$

A black hole solution in this case is known analytically [22]:

$$ds^2 = \frac{L^2}{z^2}\left(-a^2 f_{GB}(z)dt^2 + dx^2 + \frac{dz^2}{f_{GB}(z)}\right)\,, \quad (4.3)$$

where

$$f_{GB}(z) = \frac{1}{2\lambda_{GB}}\left(1 - \sqrt{1 - 4\lambda_{GB}(1 - z^4/z_H^4)}\right)\,,$$

$$a^2 = \frac{1}{2}\left(1 + \sqrt{1 - 4\lambda_{GB}}\right)\,.$$

$$\frac{dE_{GB}}{dx} = -\frac{\sqrt{\lambda}}{2\pi}\frac{1}{z^2}\frac{\sqrt{f_{GB}(z_*)}}{a}\,.$$

The 't Hooft coupling and the temperature a

$$\sqrt{\lambda} = a^2\frac{L^2}{\alpha'}\,, \qquad T = \frac{a}{\pi z_H}\,.$$

A. Ficnar , S.Gubser, MG 2013

Current work in progress to improve Jet Holography:

GB-corrected & non-conformal R_{AA}

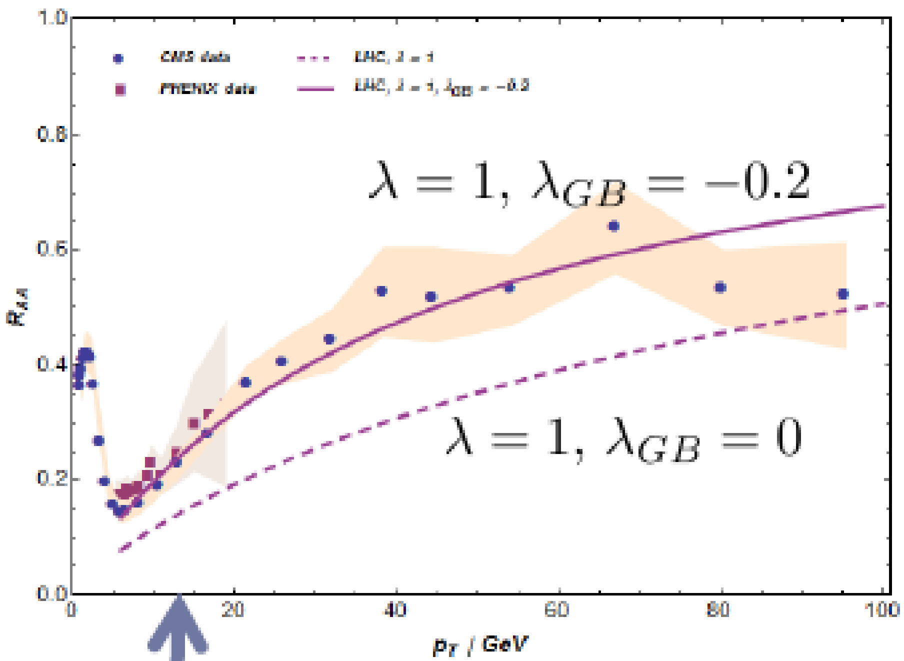

R^2 higher derivative (Gauss-Bonnet) corrections ($1/N_c$ corrections)

$$\lambda_{GB} = 0 \Rightarrow \lambda_{GB} = -0.2$$

Note

$$\frac{\eta}{s} = \frac{1}{4\pi} \Rightarrow \frac{\eta}{s} = \frac{1.8}{4\pi}$$

Non-conformal (bottom-up) deformations that fit the lattice data for thermodynamics *and* Polyakov loops ⇨ increase energy loss at low temperatures

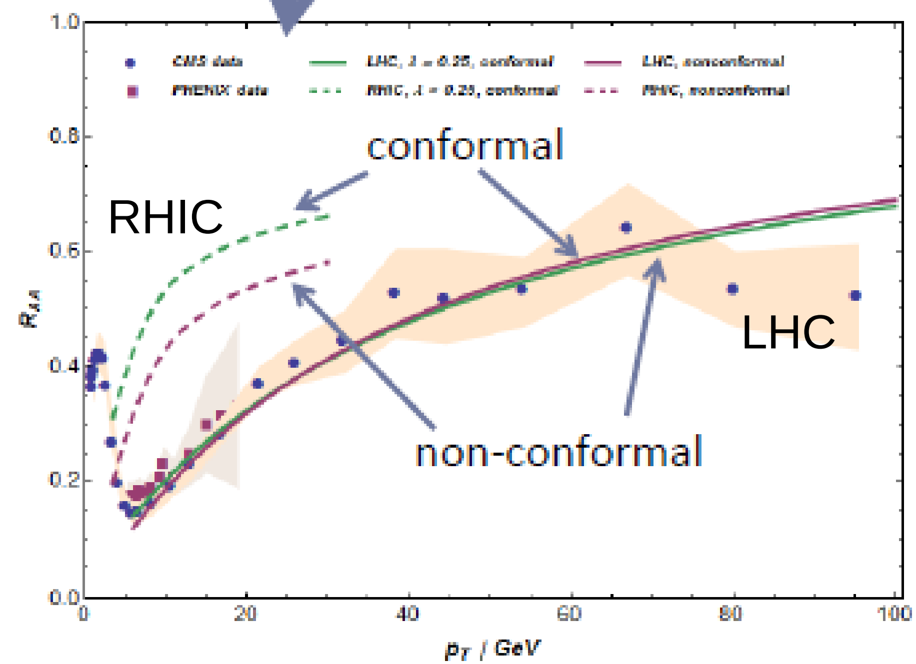

With shooting string IC, Jet Holography is finally back in the right ball park. Though convergence to data is not yet achieved

Conclusions:

1) Consistency of RHIC vs LHC Flavor Tomography/Holography is a key tool to differentiate a wide variety of weakly and strongly coupled models

2) CUJET2.0 = rcDGLV + VISH2+1 tomography results for RAA are consistent with RHIC and LHC at 2 sigma level with modest alpha_max = 0.26 +- 0.01 and HTL screening while lattice screening is not (??)

The Albatross, v2(pT), remains very challenging (despite considerable effort) and and is sensitive to *all details* of hard dE/dx as well as soft bulk QGP hydro fields

3) A new “Shooting String” Holography was proposed to overcome past failures of Falling String and String Drag models especially wrt to LHC data with lambda_tH>1

Non-conformal + Gauss Bonnet R^2 are however needed to account for the surprising similarity of RHIC and LHC data on RAA(pT, MQ, s)

and the apparent “Half Perfectness” (eta/s ~ 2X(1/4pi)) of LHC QGP flow